Spin-Orbital Entanglement in Mott Insulators

Andrzej M. Oleś
Institute of Theoretical Physics
Jagiellonian University

für Festkörperforschung

1 Entangled superexchange: SU(2) ⊗ SU(2) model **2**
1.1 Spin-orbital Hilbert space in a Mott insulator 2
1.2 Modifications due to finite spin-orbit coupling λ 3

2 Orbital physics for partly filled e_g orbitals **5**

3 Coulomb interactions in spin-orbital Hilbert space **9**
3.1 Kanamori parameters: Coulomb U and Hund's exchange J 9
3.2 Goodenough-Kanamori rules 14

4 Kugel-Khomskii model for Mott insulators **16**
4.1 Kugel-Khomskii model: 3D for $KCuF_3$ and 2D for K_2CuF_4 16
4.2 Entanglement in the ferromagnetic excitations of K_2CuF_4 20
4.3 Weak spin-orbital entanglement for large spins $S{=}2$ in $LaMnO_3$ 22

5 Spin-orbital entanglement in t_{2g} electron models **24**
5.1 Entangled phases of $LaVO_3$ and YVO_3 24
5.2 Spin-orbital entanglement on a triangular lattice 27

6 Experimental consequences of spin-orbital entanglement **30**

7 Summary **31**

Outline

Motivation: spin-orbital physics

Orbital models: ***quantum frustration***

e_g orbital model & spin order: thermodynamic order at $T<T_c$

Kugel-Khomskii model in $KCuF_3$ and K_2CuF_4

t_{2g} orbital models: $LaVO_3$, triangular lattice, Kitaev …

Experimental manifestations of entanglement

Mosaic from 12th century, Veneto
Cattedrale di San Giusto, Trieste

Thanks to:

- **Wojciech Brzezicki** Jagiellonian University, Krakow, Poland
- **Jacek Dziarmaga** Jagiellonian University, Krakow, Poland
- **Dorota Gotfryd** University of Warsaw, Warsaw, Poland
- **Mateusz Snamina** Jagiellonian University, Krakow, Poland
- **Krzysztof Wohlfeld** University of Warsaw, Warsaw, Poland
- **Lou-Fe' Feiner** Technical University, Eindhoven, Netherlands
- **Peter Horsch** Max-Planck-Institut FKF, Stuttgart, Germany
- **Giniyat Khaliullin** Max-Planck-Institut FKF, Stuttgart, Germany
- **Adolfo Avella** Universita degli Studi di Salerno, Italy
- **Mario Cuoco** Universita degli Studi di Salerno, Italy

Interplay of **spin, orbital**, charge, lattice degree of freedom

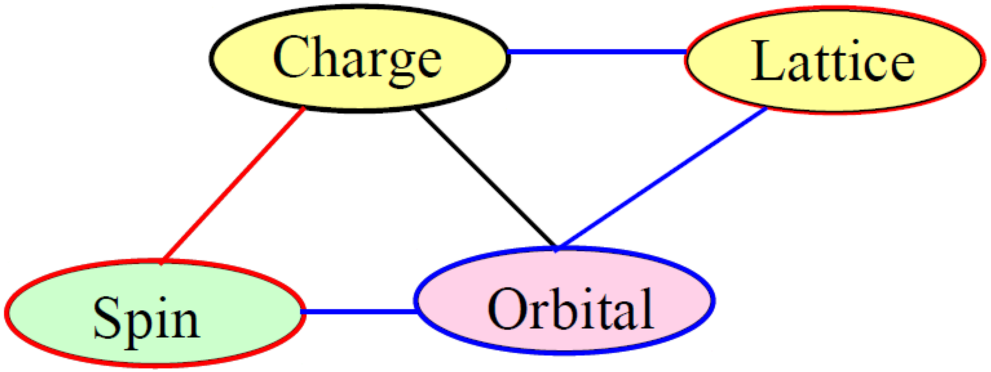

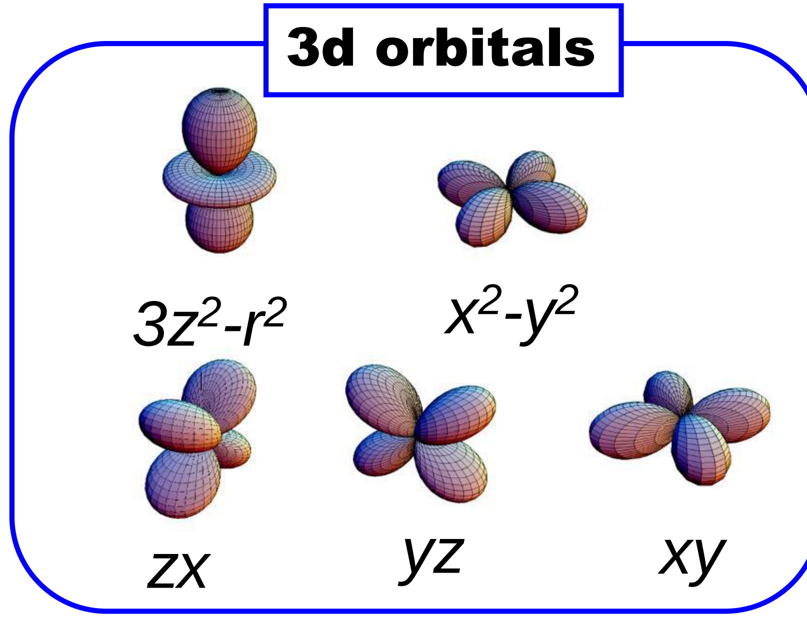

correlated insulators

orbitals are quantum

- Superconductivity
- Colossal magnetoresistance (CMR)
- Charge and orbital ordering
- Non-Fermi liquid

Inventors of spin-orbital physics at Blois (*France, 2006*)

[4] K.I. Kugel and D.I. Khomskii, Sov. Phys. Usp. **25**, 231 (1982)

Intrinsic frustration of orbital interactions due to directionality

SU(2) symmetry: $H_{spin} = J\sum_{<ij>} \vec{S}_i \bullet \vec{S}_j$

e_g systems **(** ***d^7,d^9*** **)** *z*-like active

t_{2g} systems (***d^1***, ***d^2, d^4***) two active orbitals along each axis, e.g. *zx* and *xy* along *a* axis

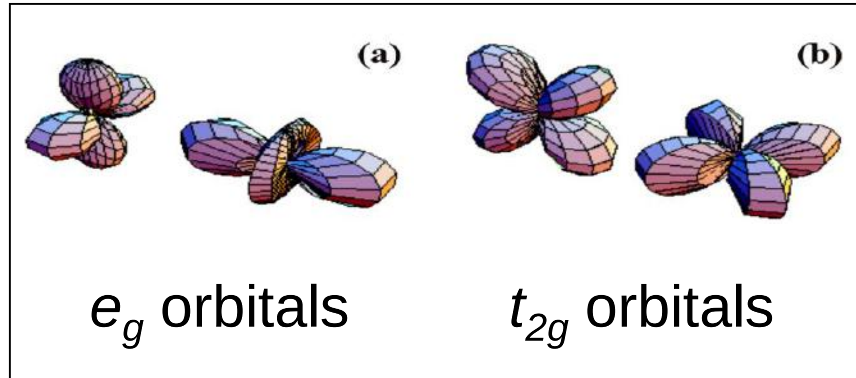

Orbital interactions are directional **!**

frustrated kagome lattice

spins:

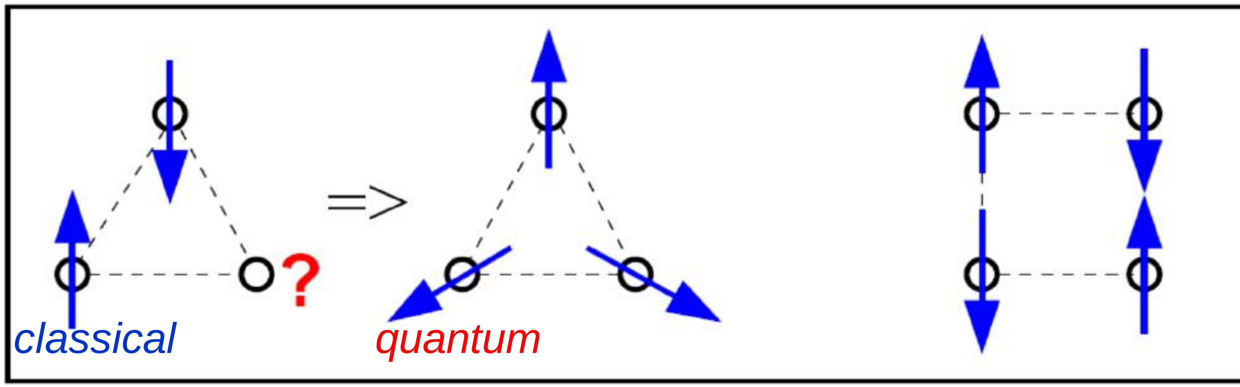

disorder: frustrated lattice

order out of disorder

square lattice: no frustration

Cubic symmetry of directional orbital interactions: $\boxed{H_{orb} = J\sum_{<ij>} T_i^{(\gamma)} T_j^{(\gamma)}}$

Interaction depends on the bond direction => ***frustration*** on a square lattice

Spin-orbital physics

AF phases with some **FM** bonds

C-AF

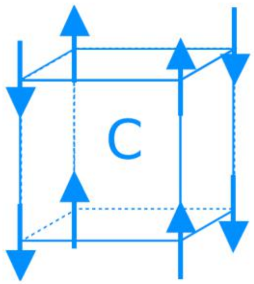

A-AF

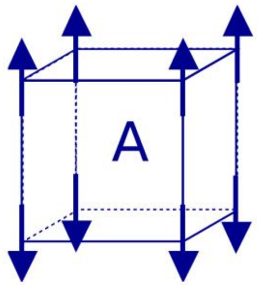

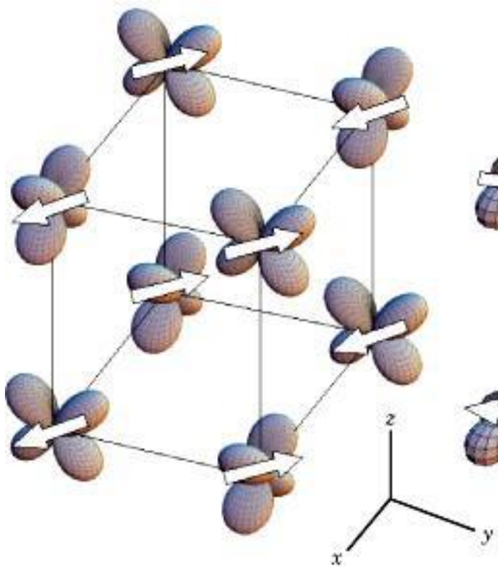

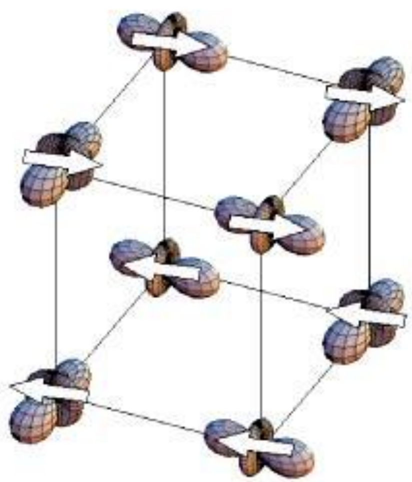

$LaVO_3$

t_{2g} orbitals

$LaMnO_3$

e_g orbitals

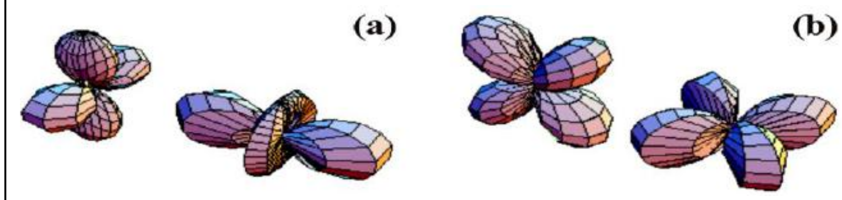

e_g orbitals t_{2g} orbitals

Orbital interactions are directional **!**

Frustration can be removed

Goodenough-Kanamori rules:

AO order supports **FM** spin order

FO order supports **AF** spin order

Are these rules sufficient?

spin-orbital entanglement

no entanglement for FM bonds

[AMO, J. Phys.: Condensed Matter **24**, 313201 (12)]

Entanglement entropy (Bipartite)

$$\mathcal{H} = \mathcal{H}_A \otimes \mathcal{H}_B$$

- Two subsystems: ***A*** and ***B***
- Wave function: $\psi_{AB} = \sum_{mn} C_{mn} \psi_A^{(m)} \psi_B^{(n)}$
- Product state: $C_{mn} = C_m C_n$
- Entangled state: $C_{mn} \neq C_m C_n$
- Taking trace over ***B*** leads to

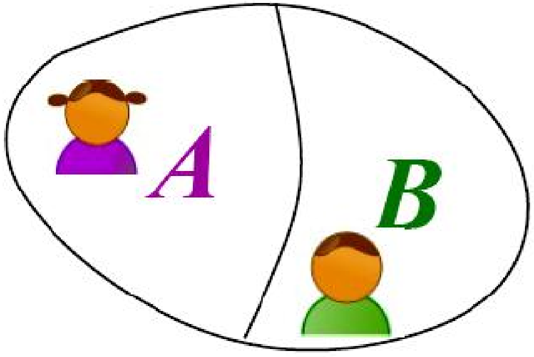

$$\rho_A^{(0)} = \mathrm{Tr}_B |\Psi_0\rangle\langle\Psi_0|$$

Entanglement is measured by von Neumann entropy in the ground state

$$S_{\mathrm{vN}}^0 \equiv -\mathrm{Tr}_A \{\rho_A^{(0)} \log_2 \rho_A^{(0)}\}$$

Here ***A* and *B*** are **spin and orbital** degrees of freedom of the system

1D entangled spin-orbital model

To illustrate these concepts, we begin with a study of a one-dimensional (1D) spin-orbital superexchange model $\mathcal{H}_{\rm SE}$ defined in a Mott insulator with on-site repulsion U by the spin-orbital Hilbert space spanned by the eigenstates $\{|\uparrow\rangle, |\downarrow\rangle\}$, of spin $S = 1/2$, and orbital (pseudospin) operator $T = 1/2$, with the eigenstates $\{|+\rangle, |-\rangle\}$. Such states at two neighboring sites i and $i+1$ are coupled by 1D spin-orbital ('Kugel-Khomskii') superexchange [4–6],

$$\mathcal{H}_{\rm SE} = J\sum_i \left[(\mathbf{S}_i \cdot \mathbf{S}_{i+1} + \alpha)(\mathbf{T}_i \cdot \mathbf{T}_{i+1} + \beta) - \alpha\beta + \varepsilon_z \sum_i \tau_i^{(c)} \right], \tag{1}$$

where $\tau_i^{(c)} = T_i^{(c)} = \sigma_i^z/2$, and we take the orbital splitting $J\varepsilon_z = E_z = 0$.

antiferromagnetic (AF) superexchange $\boxed{J = \frac{4t^2}{U}.}$

A standard measure of entanglement between two subsystems A and B in the ground state $|{\rm GS}\rangle$ of a system of size L is the von Neumann entropy [13]: $\mathcal{S}_{\rm vN} = -{\rm Tr}_A\{\rho_A \ln \rho_A\}/L$, see Fig. 1. Here our two subsystems are spins and orbitals and the entanglement concerns the entire system (in other applications the system would frequently be separated into A and B by cutting one bond). The von Neumann entropy is obtained by integrating the density matrix, $\rho_A = {\rm Tr}_B|{\rm GS}\rangle\langle{\rm GS}|$ over subsystem B. Consequently, we use here the following definition of the von Neumann spin-orbital entanglement entropy:

$$\mathcal{S}_{\rm vN} = -\frac{1}{L}{\rm Tr}_S\{\rho_S \ln \rho_S\}, \tag{3}$$

Phase diagram of the 1D spin-orbital model

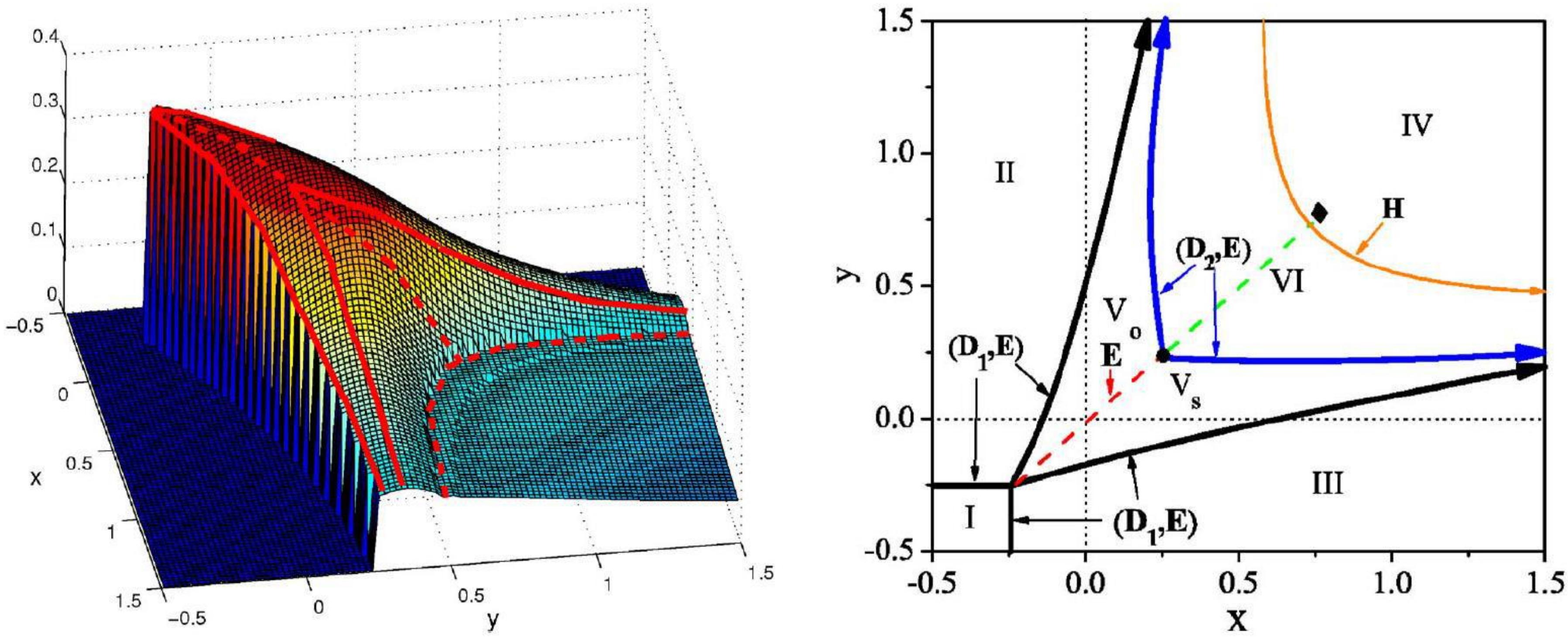

Fig. 1: *Spin-orbital entanglement in the 1D SU(2) $\otimes$ SU(2) model (1) at $E_z = 0$. Left—The von Neumann entropy per site $\mathcal{S}_{vN}/L$ (3) for the ground state at $L = 8$ as a function of x and y. The phase boundaries (solid and dashed lines) are drawn to guide the eye. Right—Phase diagram of a coupled 1D spin-orbital chain. The diamond point is located at $(^3/_4, {}^3/_4)$. Quantum phases are distinguished by entanglement: I, II, and III are disentangled, IV is weakly, and V& VI stronger entangled. The parameters (x, y) are the same as (α, β) in Fig. 2. Images after Ref. [6].*

Evolution of the 1D spin-orbital model for increasing spin-orbit coupling

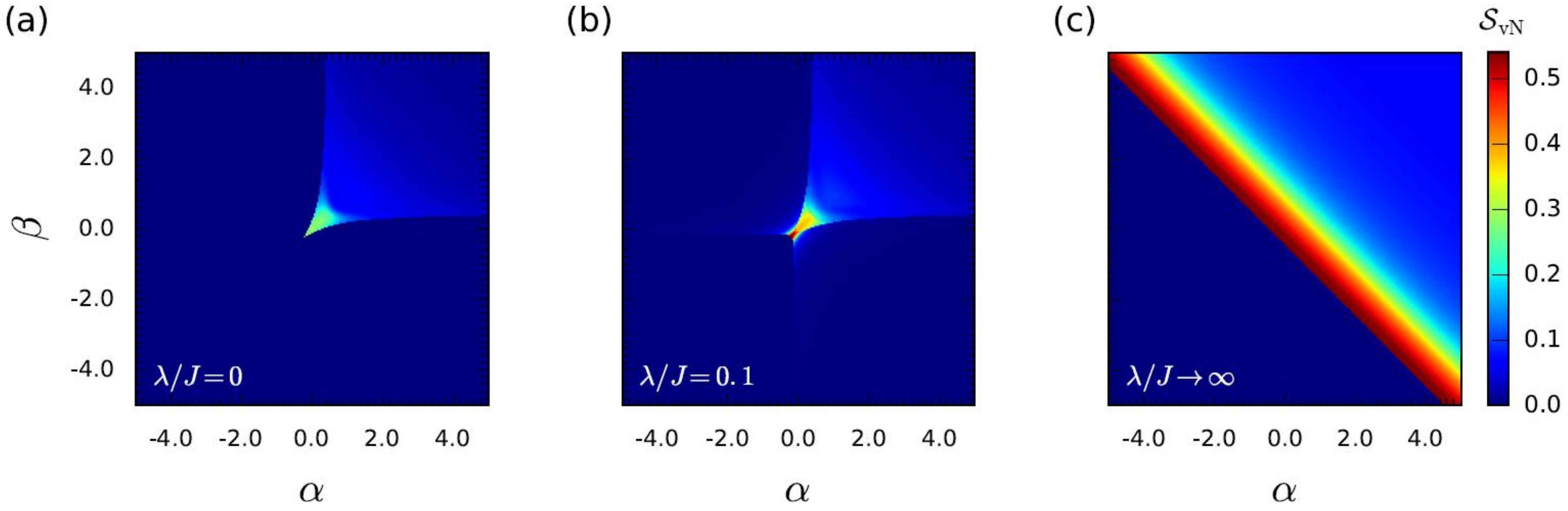

Fig. 2: *The von Neumann spin-orbital entanglement entropy,* $\mathcal{S}_{\rm vN}$ *(3), calculated using ED on an* $L{=}12$*-site periodic chain for the spin-orbital model Eq. (5) and for the increasing value of the spin-orbit coupling* λ *[15]: (a)* $\lambda/J=0$*, (b)* $\lambda/J=0.1$*, and (c)* $\lambda/J\to\infty$.

third parameter:

on-site spin-orbit coupling (SOC)

$$\boxed{\mathcal{H}_{\rm SOC}=2\lambda\sum_i S_i^z T_i^z}$$

From on-site to on-bond entanglement in spin-orbital model

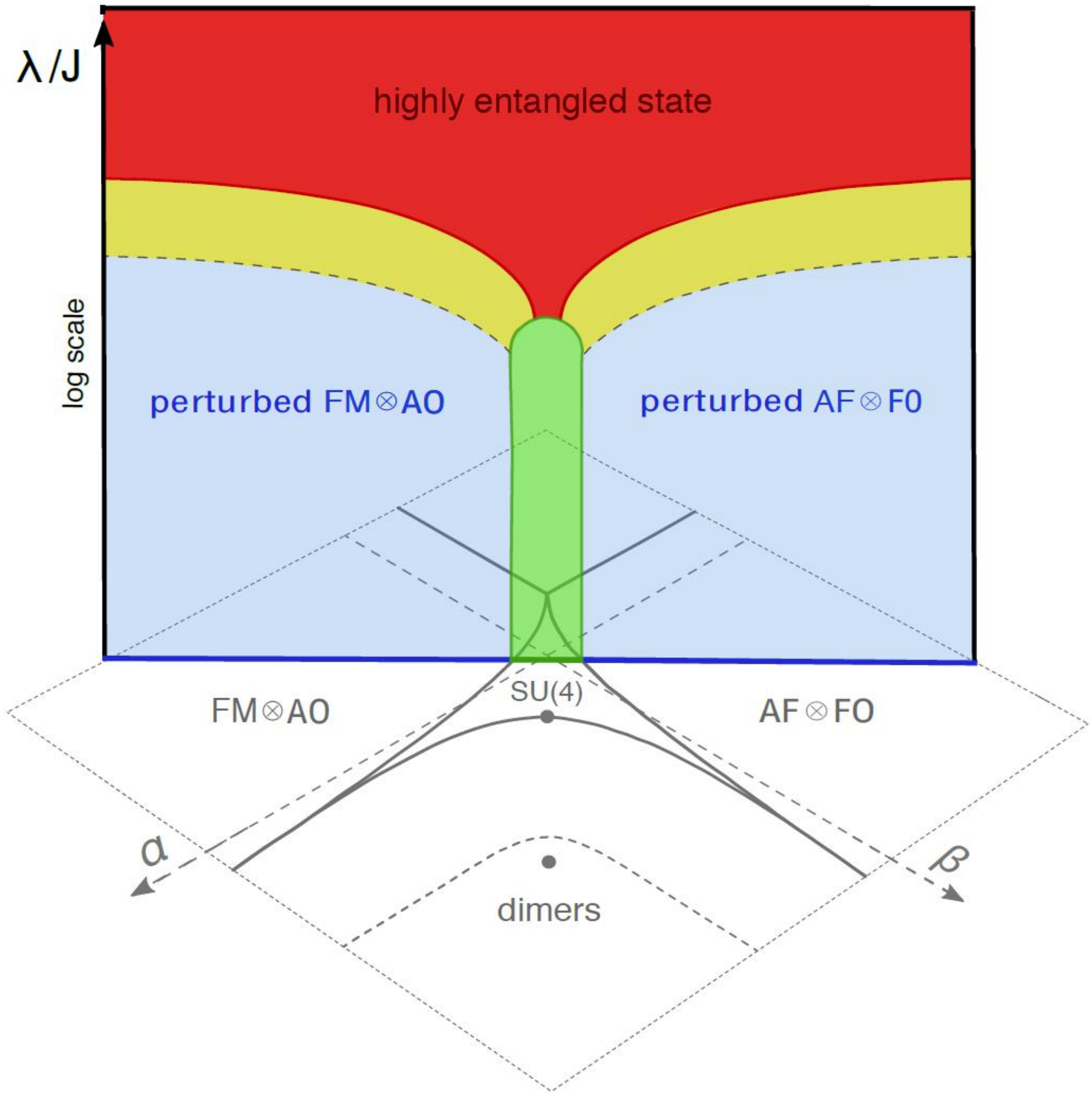

Fig. 3: *Schematic quantum phase diagram of Hamiltonian (1) in the (α, β) plane, see Fig. 1. The colorful vertical plane shows how spin-orbital entanglement extends to the highly entangled state, with on-bond entanglement in two disentangled phases: FM⊗AO and AF⊗FO, see Fig. 2.*

Hopping and orbital superexchange for t_{2g}

In **t_{2g} systems** (***d^1,d^2, …***) two states

are active along each cubic axis,
e.g. *yz* & *zx* for the axis *c* –

$$H_t(t_{2g}) = -t \sum_{\alpha} \sum_{\langle ij\rangle \| \gamma \neq \alpha} a^{\dagger}_{i\alpha\sigma} a_{j\alpha\sigma}$$

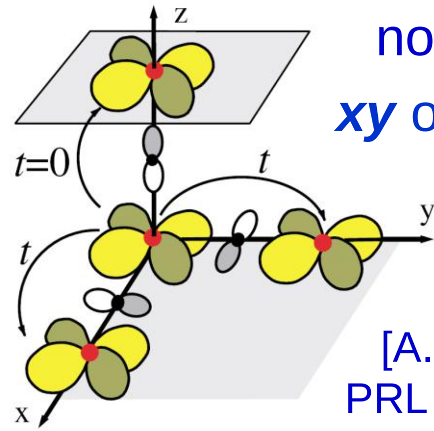

no hopping ||*c*

xy orbital called ***c***

[A.B. Harris *et al*., PRL **91**, 087206 (03)]

We introduce convenient notation

$$|a\rangle \equiv |yz\rangle, \qquad |b\rangle \equiv |zx\rangle, \qquad |c\rangle \equiv |xy\rangle$$

Orbital interactions have cubic symmetry

they are described by **quantum** operators:

$$\vec{T}_i = \{T_i^x, T_i^y, T_i^z\} \qquad T_i^x = \frac{1}{2}\sigma_i^x,\ T_i^y = \frac{1}{2}\sigma_i^y,\ T_i^z = \frac{1}{2}\sigma_i^z.$$

Scalar product $\vec{T}_i \cdot \vec{T}_j$ but for J_H>0 also other terms breaking the „SU(2)” symmetry

Orbital Hubbard model for e_g orbitals

Hamiltonian for e_g electrons couples two directional e_g-orbitals

Real basis:

$$H_t(e_g) = -t \sum_{\alpha} \sum_{\langle ij \rangle \| \alpha, \sigma} a^{\dagger}_{i\zeta_\alpha \sigma} a_{j\zeta_\alpha \sigma}$$

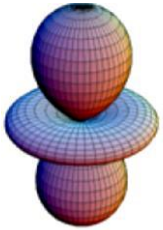

$$|z\rangle \equiv \frac{1}{\sqrt{6}}(3z^2 - r^2), \qquad |\bar{z}\rangle \equiv \frac{1}{\sqrt{2}}(x^2 - y^2)$$

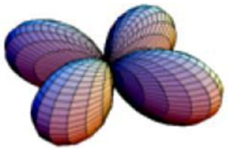

$$H_t^{\uparrow}(e_g) = -\frac{1}{4} t \sum_{\langle ij \rangle \| ab} \left[3a^{\dagger}_{i\bar{z}} a_{j\bar{z}} + a^{\dagger}_{iz} a_{jz} \mp \sqrt{3} \left(a^{\dagger}_{i\bar{z}} a_{jz} + a^{\dagger}_{iz} a_{j\bar{z}} \right) \right] - t \sum_{\langle ij \rangle \| c} a^{\dagger}_{iz} a_{jz}$$

complex e_g orbitals

$$|j+\rangle = \frac{1}{\sqrt{2}}(|jz\rangle - i|j\bar{z}\rangle), \qquad |j-\rangle = \frac{1}{\sqrt{2}}(|jz\rangle + i|j\bar{z}\rangle)$$

$$\mathcal{H}^{\uparrow}(e_g) = -\frac{1}{2} t \sum_{\alpha} \sum_{\langle ij \rangle \| \alpha} \left[\left(a^{\dagger}_{i+} a_{j+} + a^{\dagger}_{i-} a_{j-} \right) + \gamma \left(e^{-i\chi_\alpha} a^{\dagger}_{i+} a_{j-} + e^{+i\chi_\alpha} a^{\dagger}_{i-} a_{j+} \right) \right]$$

with $\chi_a = +2\pi/3$, $\chi_b = -2\pi/3$, and $\chi_c = 0$ has cubic symmetry

with interaction $\bar{U} \sum_i n_{i+} n_{i-}$ => *orbital Hubbard model*

Orbital models

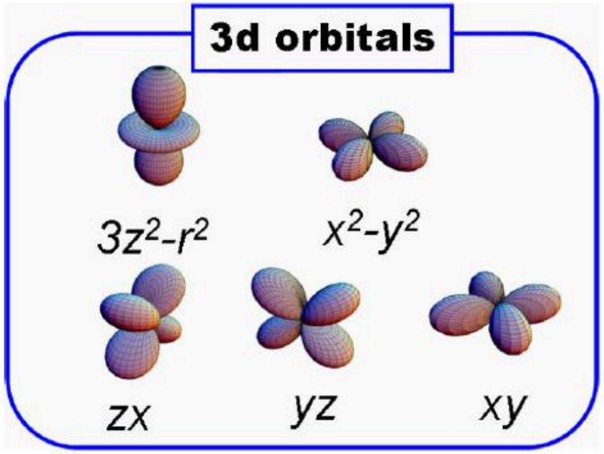

t_{2g} orbitals: $|a\rangle \equiv |yz\rangle, \qquad |b\rangle \equiv |zx\rangle, \qquad |c\rangle \equiv |xy\rangle.$

$$H_t(t_{2g}) = -t \sum_{\alpha} \sum_{\langle ij\rangle \parallel \gamma \neq \alpha} a^{\dagger}_{i\alpha\sigma} a_{j\alpha\sigma},$$

e_g orbitals: $|z\rangle \equiv \frac{1}{\sqrt{6}}|3z^2-r^2\rangle, \qquad |\bar{z}\rangle \equiv \frac{1}{\sqrt{2}}|x^2-y^2\rangle,$

$$H_t(e_g) = -t \sum_{\alpha} \sum_{\langle ij\rangle \parallel \alpha,\sigma} a^{\dagger}_{i\zeta_\alpha\sigma} a_{j\zeta_\alpha\sigma}.$$

real orbitals

$$H_t^{\uparrow}(e_g) = -\frac{1}{4}t \sum_{\langle mn\rangle \parallel ab} \left[3a^{\dagger}_{i\bar{z}}a_{j\bar{z}} + a^{\dagger}_{iz}a_{jz} \mp \sqrt{3}\left(a^{\dagger}_{i\bar{z}}a_{jz} + a^{\dagger}_{iz}a_{j\bar{z}}\right)\right] - t \sum_{\langle ij\rangle \parallel c} a^{\dagger}_{iz}a_{jz}. \qquad (11)$$

More symmetric for **complex orbitals** with orbital phases

$$|i+\rangle = \frac{1}{\sqrt{2}}(|iz\rangle - \mathrm{i}\,|i\bar{z}\rangle), \qquad |i-\rangle = \frac{1}{\sqrt{2}}(|iz\rangle + \mathrm{i}\,|i\bar{z}\rangle),$$

$$\mathcal{H}_{e_g}^{\uparrow} = -\frac{t}{2}\sum_{\gamma}\sum_{\langle ij\rangle\parallel\gamma}\left[\left(a^{\dagger}_{i+}a_{j+} + a^{\dagger}_{i-}a_{j-}\right) + \gamma\left(e^{-\mathrm{i}\chi_\gamma}a^{\dagger}_{i+}a_{j-} + e^{+\mathrm{i}\chi_\gamma}a^{\dagger}_{i-}a_{j+}\right)\right] + \bar{U}\sum_m n_{i+}n_{i-}, \quad (16)$$

with $\chi_a = +2\pi/3$, $\chi_b = -2\pi/3$, and $\chi_c = 0$

Superexchange only possible for two orbital configurations:

$$\mathcal{P}^{(\gamma)}_{\langle ij\rangle} \equiv \left(\frac{1}{2} + \tau_i^{(\gamma)}\right)\left(\frac{1}{2} - \tau_j^{(\gamma)}\right) + \left(\frac{1}{2} - \tau_i^{(\gamma)}\right)\left(\frac{1}{2} + \tau_j^{(\gamma)}\right), \qquad (17)$$

$$\mathcal{Q}^{(\gamma)}_{\langle ij\rangle} \equiv 2\left(\frac{1}{2} - \tau_i^{(\gamma)}\right)\left(\frac{1}{2} - \tau_j^{(\gamma)}\right). \qquad (18)$$

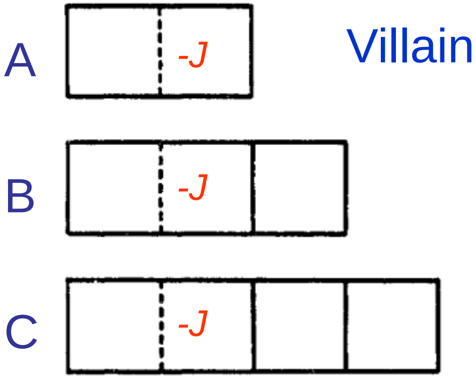

2D order in e_g orbital model

$$T_c^{\text{Ising}} = \frac{1}{2\log(1+\sqrt{2})} \approx 0.567296.$$

[L. Longa, AMO, J. Phys. A **13**, 1031 (80)]

TABLE I. The critical temperature $\mathcal{T}_c$ and the type of order for the classical and quantum models on a square lattice: Ising model, $\frac{1}{2}$ and $\frac{2}{3}$ frustrated Ising [29], fully frustrated Villain model [30], e_g orbital model [23] and 2D compass model [22].

2D model	order	$\mathcal{T}_c/J$	method	interactions
Ising	2D	0.567296	exact	Onsager
$\frac{1}{2}$ frustrated	2D	0.410	exact	C
$\frac{2}{3}$ frustrated	2D	0.342	exact	B
Villain	—	0.0	exact	A
e_g orbital	2D	0.3566 ± 0.0001	VTNR	$\propto \frac{3}{16}\sigma_i^x\sigma_j^x$
compass	nematic	0.0606 ± 0.0004	VTNR	$\frac{1}{4}\sigma_i^z\sigma_j^z$

e_g orbital model spinless electrons

Orbital superexchange => AO

$$|z\rangle \equiv \frac{1}{\sqrt{6}}|3z^2-r^2\rangle, \qquad |\bar{z}\rangle \equiv \frac{1}{\sqrt{2}}|x^2-y^2\rangle,$$

e_g-orbital model in $d = \infty$ dimensions

Gutzwiller approximation contains mostly the OL phase

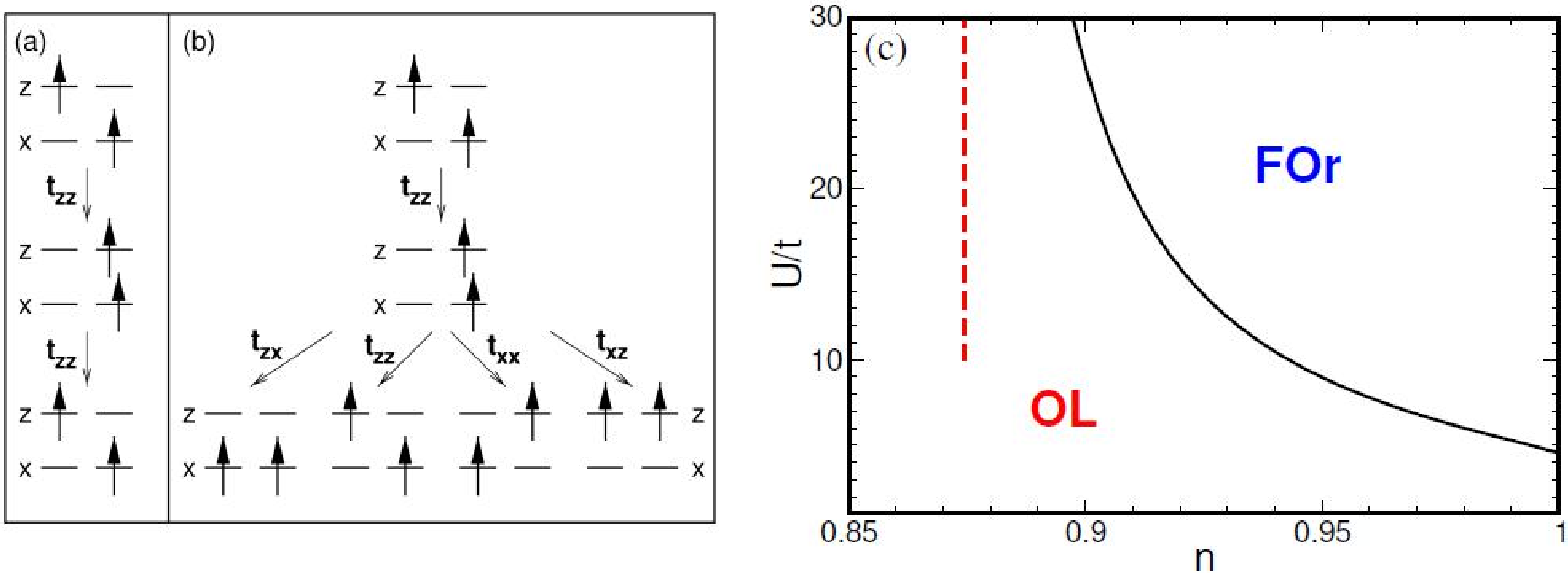

Fig. 5: *Virtual charge excitations leading to the e_g-orbital superexchange model for a strongly correlated system with $|z\rangle$ and $|x\rangle \equiv |\bar{z}\rangle$ real e_g orbitals (10) in the subspace of $\uparrow$-spin states: (a) for a bond along the c axis $\langle ij\rangle \parallel c$; (b) for a bond in the ab plane $\langle ij\rangle \parallel ab$. In a FM plane of $KCuF_3$ ($LaMnO_3$) the superexchange favors AO state of $|\mathrm{AO}\pm\rangle$ orbitals (not shown).*
(c) The transition from FOr to OL found at $d = \infty$ at finite U, and at $U = \infty$ (dashed line).

Entanglement by on-site spin-orbit: compass and Kitaev

$$\boxed{\mathcal{H}_{ij}^{(\gamma)} = -JS_i^\gamma S_j^\gamma}$$

[G. Jackeli and G. Khaliullin, PRL **102**, 017205 (09)]

Kramers doublet of entangled states:

$$|\tilde{\uparrow}\rangle = \sin\theta|0,\uparrow\rangle - \cos\theta|+1,\downarrow\rangle,$$

$$|\tilde{\downarrow}\rangle = \sin\theta|0,\downarrow\rangle - \cos\theta|-1,\uparrow\rangle.$$

t_{2g} orbitals: l =1, l_z= -1,0,+1

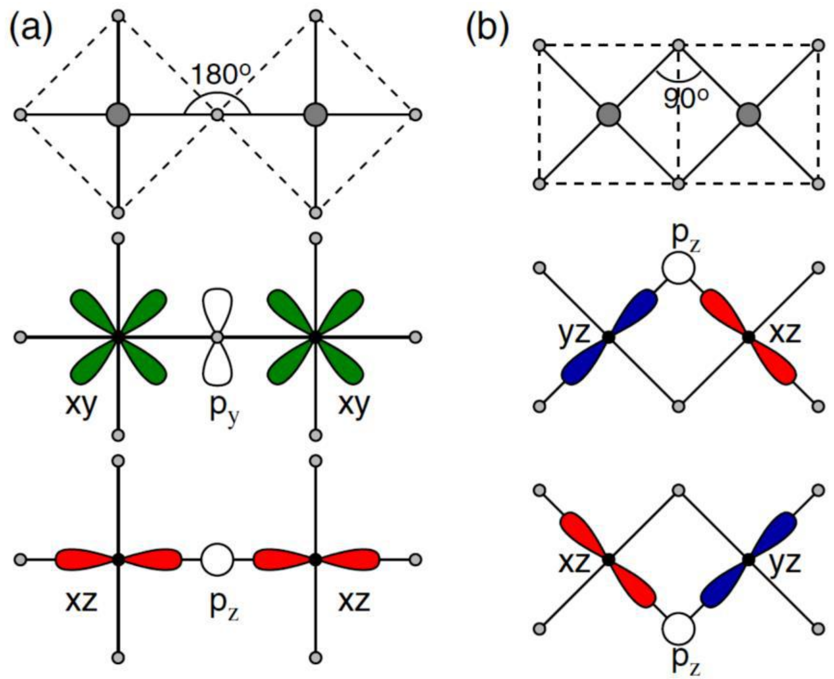

FIG. 2 (color online). Two possible geometries of a TM-O-TM bond with corresponding orbitals active along these bonds. The

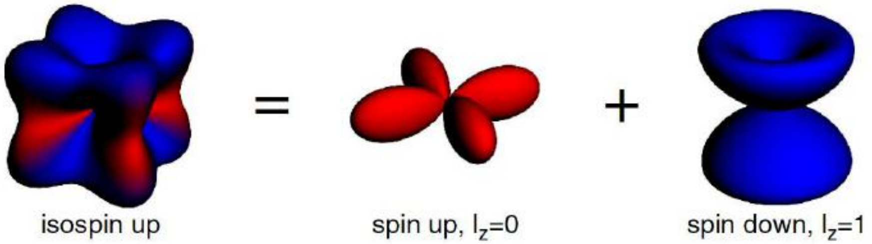

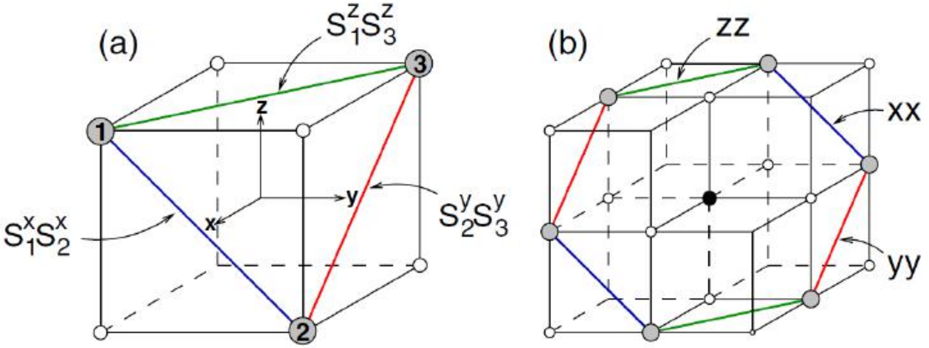

ABO_2 structure

triangular compass

A_2BO_3 structure

hexagonal Kitaev

Which kind of e_g spin-orbital order ?

Strong in-plane anisotropy for ***G*-AF**

$|z\rangle$

$|\bar{z}\rangle$

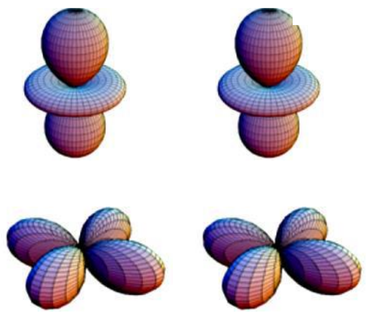

$$J_{ab}^{z} = \frac{1}{16} J$$

$$J_{ab}^{\bar{z}} = \frac{9}{16} J$$

spin exchange

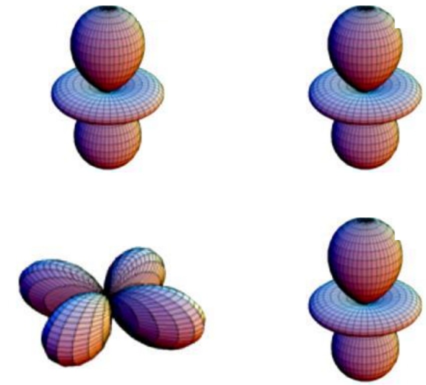

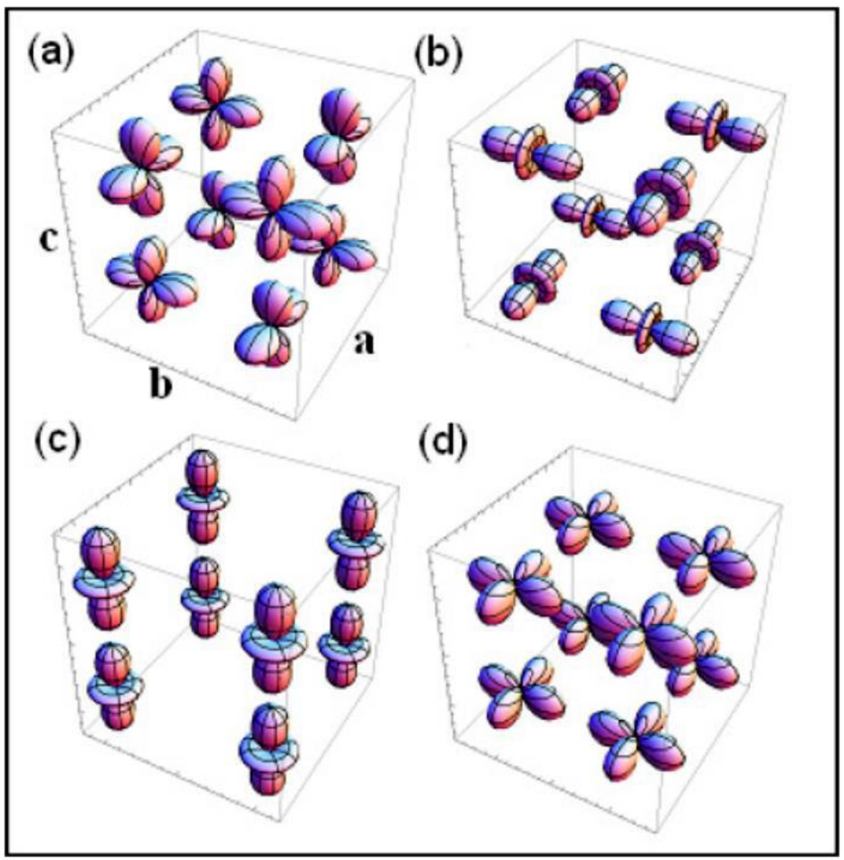

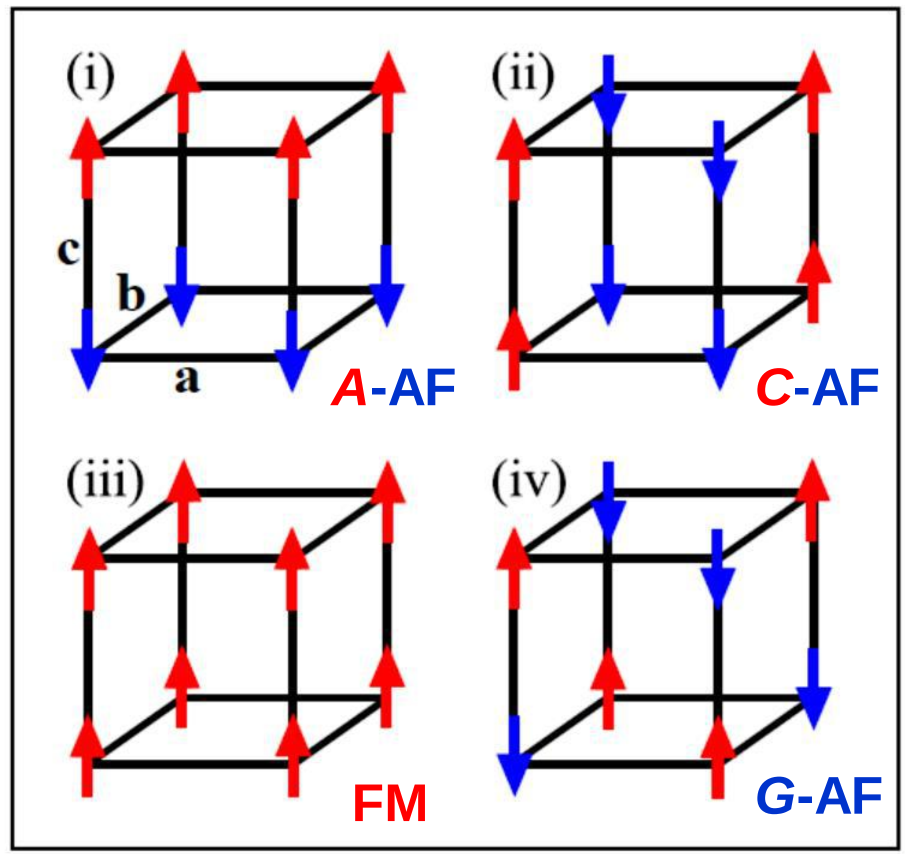

Kanamori parameters: Coulomb U and Hund's exchange J

$$
\begin{aligned}
H_{int} &= U\sum_{i\alpha} n_{i\alpha\uparrow}n_{i\alpha\downarrow} + \sum_{i,\alpha<\beta}\left(U'_{\alpha\beta} - \frac{1}{2}J_{\alpha\beta}\right) n_{i\alpha}n_{i\beta} - 2\sum_{i,\alpha<\beta} J_{\alpha\beta}\,\vec{S}_{i\alpha}\cdot\vec{S}_{i\beta} \\
&+ \sum_{i,\alpha<\beta} J_{\alpha\beta}\left(a^\dagger_{i\alpha\uparrow}a^\dagger_{i\alpha\downarrow}a_{i\beta\downarrow}a_{i\beta\uparrow} + a^\dagger_{i\beta\uparrow}a^\dagger_{i\beta\downarrow}a_{i\alpha\downarrow}a_{i\alpha\uparrow}\right). \qquad (19)
\end{aligned}
$$

$$\boxed{U \equiv A + 4B + 3C,}$$

inter-orbital exchange elements $J_{\alpha\beta}$ for 3d orbitals

$3d$ orbital	xy	yz	zx	x^2-y^2	$3z^2-r^2$
xy	0	$3B+C$	$3B+C$	C	$4B+C$
yz	$3B+C$	0	$3B+C$	$3B+C$	$B+C$
zx	$3B+C$	$3B+C$	0	$3B+C$	$B+C$
x^2-y^2	C	$3B+C$	$3B+C$	0	$4B+C$
$3z^2-r^2$	$4B+C$	$B+C$	$B+C$	$4B+C$	0

$$U = U'_{\alpha\beta} + 2J_{\alpha\beta}.$$

$$\boxed{\begin{aligned} J_H^t &\equiv 3B + C, \\ J_H^e &\equiv 4B + C. \end{aligned}}$$

degenerate Hubbard model

$$
\boxed{\begin{aligned}
H_{int}^{(0)} &= U\sum_{i\alpha} n_{i\alpha\uparrow}n_{i\alpha\downarrow} + \left(U - \frac{5}{2}J_H\right)\sum_{i,\alpha<\beta} n_{i\alpha}n_{m\beta} - 2J_H\sum_{i,\alpha<\beta}\vec{S}_{i\alpha}\cdot\vec{S}_{i\beta} \\
&+ J_H\sum_{i,\alpha<\beta}\left(a^\dagger_{i\alpha\uparrow}a^\dagger_{i\alpha\downarrow}a_{i\beta\downarrow}a_{i\beta\uparrow} + a^\dagger_{i\beta\uparrow}a^\dagger_{i\beta\downarrow}a_{i\alpha\downarrow}a_{i\alpha\uparrow}\right). \qquad (24)
\end{aligned}}
$$

Degenerate Hubbard model & charge excitations ($t << U$)

Two parameters: ***U*** – intraorbital Coulomb interaction, ***J_H*** – Hund's exchange

$$H_{\text{int}} = U\sum_{i\alpha} n_{i\alpha\uparrow}n_{i\alpha\downarrow} + (U - \tfrac{5}{2}J_H)\sum_{i,\alpha<\beta} n_{i\alpha}n_{i\beta} - 2J_H \sum_{i,\alpha<\beta} \vec{S}_{i\alpha}\cdot\vec{S}_{i\beta}$$
$$+ J_H \sum_{i,\alpha<\beta} (d^{+}_{i\alpha\uparrow}d^{+}_{i\alpha\downarrow}d_{i\beta\downarrow}d_{i\beta\uparrow} + d^{+}_{i\beta\uparrow}d^{+}_{i\beta\downarrow}d_{i\alpha\downarrow}d_{i\alpha\uparrow})$$

[A.M. Oleś, PRB **28**, 327 (1983)]

In a Mott insulator (t<<U) superexchange follows from charge excitations

$$d_i^m d_j^m \rightleftharpoons d_i^{m+1} d_j^{m-1}$$

single parameter:

$\eta = J_H/U$

e_g systems | t_{2g} systems

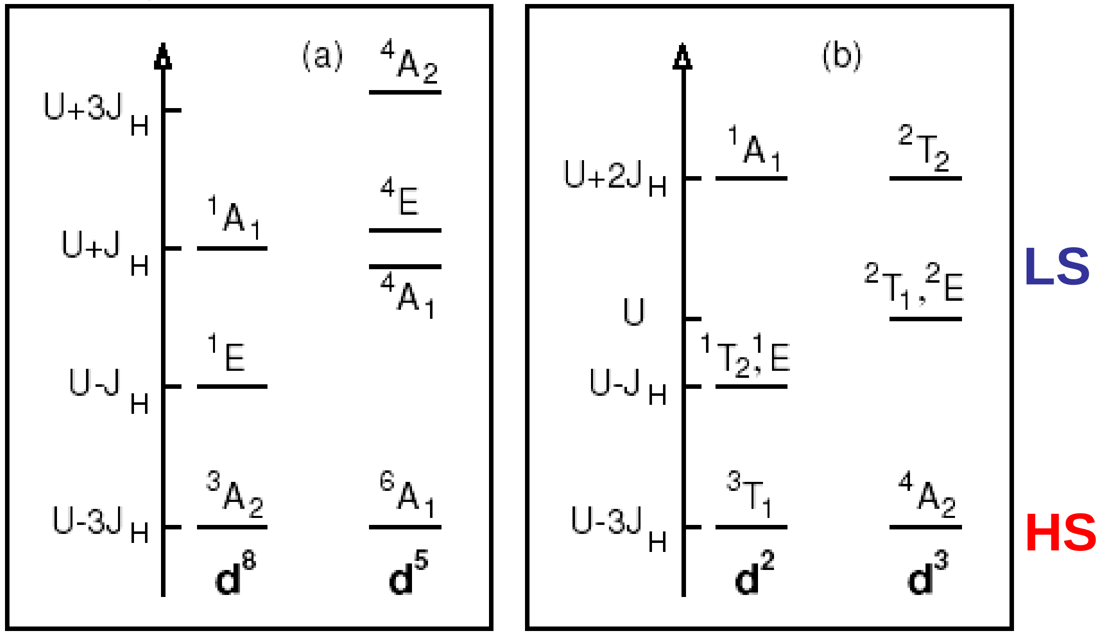

FIG. 1: Energies of $d_i^m d_j^m \to d_i^{m+1} d_j^{m-1}$ charge excitations

SOE 18 Sep

Spin-orbital superexchange model

$$\boxed{\mathcal{H} = -\sum_n \frac{t^2}{\varepsilon_n} \sum_{\langle ij\rangle \| \gamma} P_{\langle ij\rangle}(\mathcal{S})\, \mathcal{O}^{\gamma}_{\langle ij\rangle}}$$

$P_{\langle ij\rangle}(\mathcal{S})$ is the projection on the total spin $\mathcal{S} = S \pm 1/2$

Spins and orbitals are entangled

orbital operators, $\hat{\mathcal{K}}_{ij}^{(\gamma)}$ and $\hat{\mathcal{N}}_{ij}^{(\gamma)}$

$$\mathcal{H}_J = J \sum_\gamma \sum_{\langle ij\rangle \| \gamma} \left\{ \hat{\mathcal{K}}_{ij}^{(\gamma)} \left(\vec{S}_i \cdot \vec{S}_j + S^2 \right) + \hat{\mathcal{N}}_{ij}^{(\gamma)} \right\}. \tag{28}$$

anisotropic modes; spin correlations depend on direction

$$H = J_{ab} \sum_{\langle ij\rangle \| ab} \vec{S}_i \cdot \vec{S}_j + J_c \sum_{\langle ij\rangle \| c} \vec{S}_i \cdot \vec{S}_j, \tag{29}$$

$$\boxed{s_c = \left\langle \vec{S}_i \cdot \vec{S}_j \right\rangle_c, \qquad s_{ab} = \left\langle \vec{S}_i \cdot \vec{S}_j \right\rangle_{ab},}$$

Optical sum rules follow from superexchange ($t<<U$)

Spin-orbital superexchange model for a perovskite, $\gamma=a,b,c$ ($J=4t^2/U$):

$$\mathcal{H}_J = J\sum_{\gamma}\sum_{\langle ij\rangle\|\gamma}\left\{\hat{\mathcal{K}}_{ij}^{(\gamma)}\left(\vec{S}_i\cdot\vec{S}_j+S^2\right)+\hat{\mathcal{N}}_{ij}^{(\gamma)}\right\}$$

contains orbital operators, $\hat{\mathcal{K}}_{ij}^{(\gamma)}$ and $\hat{\mathcal{N}}_{ij}^{(\gamma)}$

Kinetic energy determined by charge excitation n along $\gamma=a,b,c$:

$$\boxed{K_n^{(\gamma)} = -2\left\langle H_n^{(\gamma)}(ij)\right\rangle = \frac{2}{\pi}\frac{a_0\hbar^2}{e^2}\int_0^\infty \sigma_n^{(\gamma)}(\omega)\,d\omega}$$

Superexchange determines **partial optical sum rule** for individual subband n:

$$\boxed{N_{\mathrm{eff},n}^{(\gamma)} = -\frac{m_0a_0^2}{\hbar^2}K_n^{(\gamma)} = -\frac{m_0a_0^2}{\hbar^2}\langle 2H_n^{(\gamma)}(ij)\rangle}$$

Each multiplet level n represents an upper Hubbard subband

Can spin and orbital operators be **disentangled ?**

[G. Khaliullin, P. Horsch, AMO, PRB **70**, 195103 (04)]

Goodenough-Kanamori rules

AF SO has as well FO order, while FM SO is accompanied by AO order.

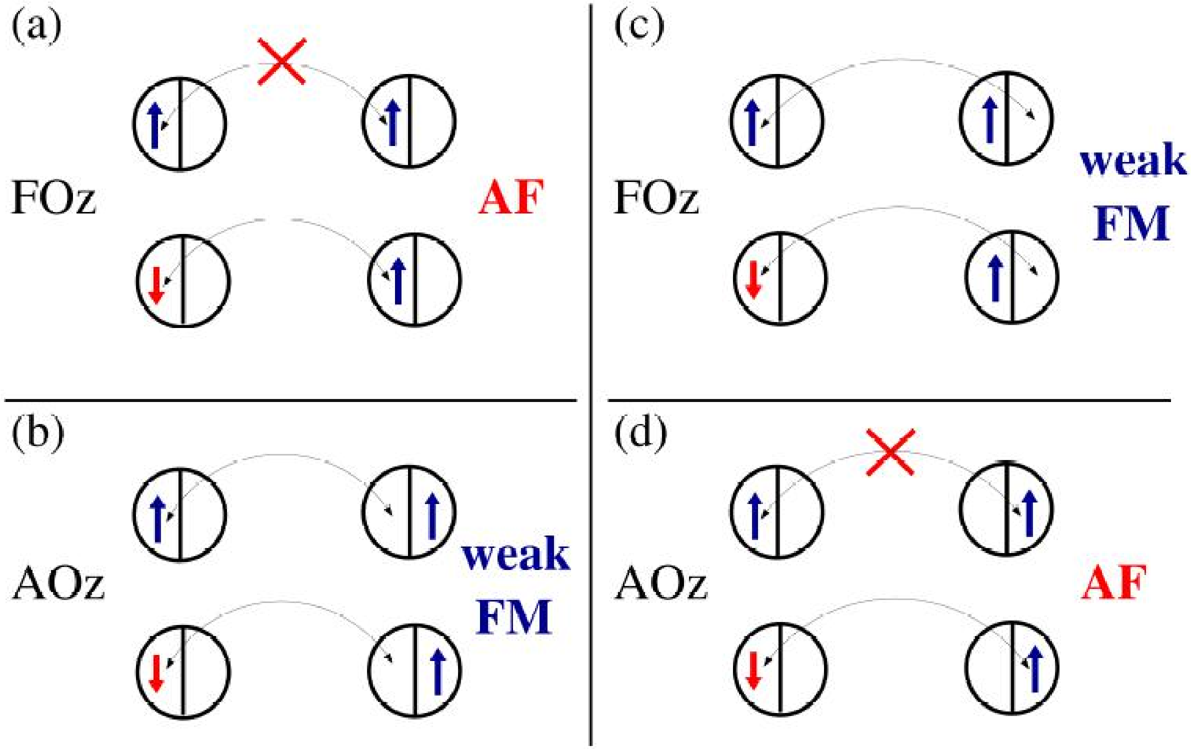

Fig. 7: *Artist's view of the GKR [36] for: (a) FOz and AF spin order and (b) AOz and FM spin order in a system with orbital flavor conserving hopping as alkali RO_2 hyperoxides ($R = K, Rb, Cs$) [38]. The charge excitations generated by inter-orbital hopping fully violate the GKR and support the states with the same spin-orbital order: (c) FOz and FM spin order and (d) AOz and AF spin order. Image reproduced from Ref. [38].*

Disentanglement: Spinon-orbiton separation

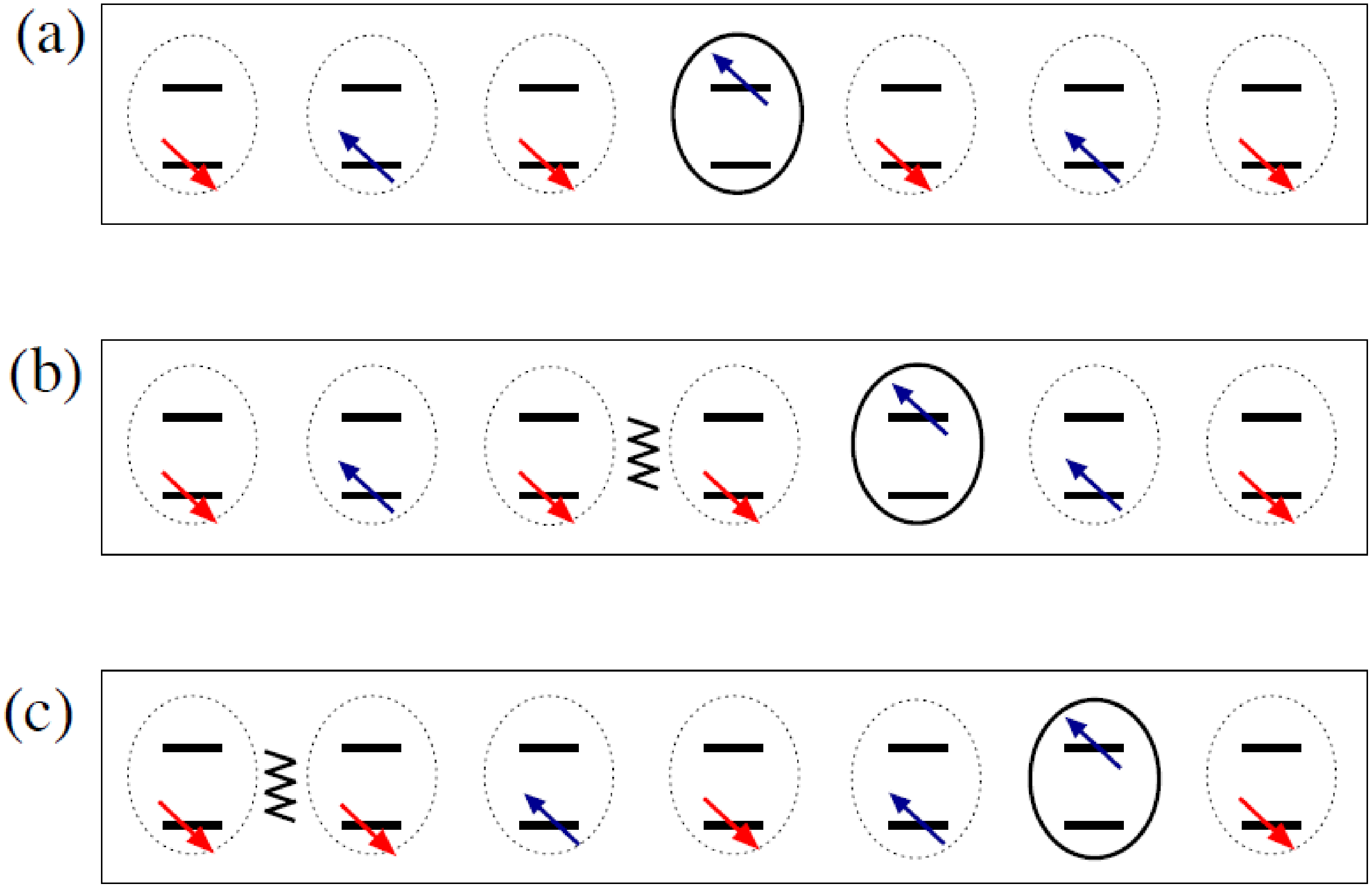

Fig. 8: *Schematic representation of the orbital motion and the spin-orbital separation in a 1D spin-orbital model. The first hop of the excited state (a)→(b) creates a spinon (wavy line) that moves via spin exchange $\propto J$. The next hop (b)→(c) gives an "orbiton" freely propagating as a "holon" with an effective hopping $t \sim J/2$. Image reproduced from Ref. [39].*

Kugel-Khomskii model

$$d_i^9 d_j^9 \rightleftharpoons d_i^{10} d_j^8$$

We follow the general scheme:

$$\mathcal{H} = -\sum_n \frac{t^2}{\varepsilon_n} \sum_{\langle ij\rangle \| \gamma} P_{\langle ij\rangle}(\mathcal{S})\, \mathcal{O}^{\gamma}_{\langle ij\rangle}$$

$$\begin{aligned}\mathcal{H}(d^9) \;=\; & \sum_\gamma \sum_{\langle ij\rangle\|\gamma} \Bigg\{ -\frac{t^2}{U-3J_H}\left(\vec{S}_i\cdot\vec{S}_j+\frac{3}{4}\right)\mathcal{P}^{(\gamma)}_{\langle ij\rangle} + \frac{t^2}{U-J_H}\left(\vec{S}_i\cdot\vec{S}_j-\frac{1}{4}\right)\mathcal{P}^{(\gamma)}_{\langle ij\rangle} \\ & + \left(\frac{t^2}{U-J_H}+\frac{t^2}{U+J_H}\right)\left(\vec{S}_i\cdot\vec{S}_j-\frac{1}{4}\right)\mathcal{Q}^{(\gamma)}_{\langle ij\rangle}\Bigg\} + E_z\sum_i \tau_i^c . \qquad (44)\end{aligned}$$

KK model

crystal field $\propto E_z$

with

$$\mathcal{P}^{(\gamma)}_{\langle ij\rangle} \equiv \left(\frac{1}{2}+\tau_i^{(\gamma)}\right)\left(\frac{1}{2}-\tau_j^{(\gamma)}\right)+\left(\frac{1}{2}-\tau_i^{(\gamma)}\right)\left(\frac{1}{2}+\tau_j^{(\gamma)}\right),$$

$$\mathcal{Q}^{(\gamma)}_{\langle ij\rangle} \equiv 2\left(\frac{1}{2}-\tau_i^{(\gamma)}\right)\left(\frac{1}{2}-\tau_j^{(\gamma)}\right).$$

ε_n

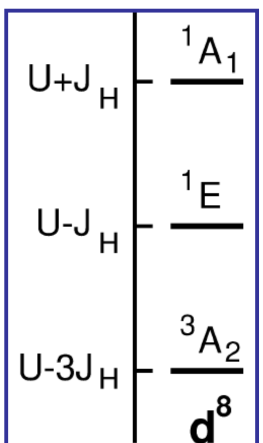

charge excitation			spin state		orbital state	
n	type	ε_n	$\mathcal{S}$	$P_{\langle ij\rangle}(\mathcal{S})$	orbitals on $\langle ij\rangle \parallel \gamma$	projection
1	HS	$U-3J_H$	1	$\left(\vec{S}_i\cdot\vec{S}_j+\frac{3}{4}\right)$	$\lvert i\zeta_\gamma\rangle\lvert j\xi_\gamma\rangle\;(\lvert i\xi_\gamma\rangle\lvert j\zeta_\gamma\rangle)$	$\mathcal{P}^{(\gamma)}_{\langle ij\rangle}$
2	LS	$U-J_H$	0	$-\left(\vec{S}_i\cdot\vec{S}_j-\frac{1}{4}\right)$	$\lvert i\zeta_\gamma\rangle\lvert j\xi_\gamma\rangle\;(\lvert i\xi_\gamma\rangle\lvert j\zeta_\gamma\rangle)$	$\mathcal{P}^{(\gamma)}_{\langle ij\rangle}$
3	LS	$U-J_H$	0	$-\left(\vec{S}_i\cdot\vec{S}_j-\frac{1}{4}\right)$	$\lvert i\zeta_\gamma\rangle\lvert j\zeta_\gamma\rangle$	$\mathcal{Q}^{(\gamma)}_{\langle ij\rangle}$
4	LS	$U+J_H$	0	$-\left(\vec{S}_i\cdot\vec{S}_j-\frac{1}{4}\right)$	$\lvert i\zeta_\gamma\rangle\lvert j\zeta_\gamma\rangle$	$\mathcal{Q}^{(\gamma)}_{\langle ij\rangle}$

Kugel-Khomskii model

Equidistant multiplet structure for d^8 ions

$\eta = J_H/U$

Charge excitations fully characterized by:

$$r_1 = \frac{1}{1-3\eta}, \qquad r_2 = r_3 = \frac{1}{1-\eta}, \qquad r_4 = \frac{1}{1+\eta}$$

$J = 4t^2/U$

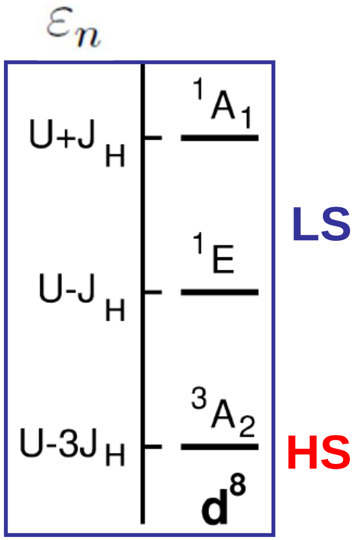

$$\mathcal{H}(d^9) = \frac{1}{2}J\sum_{\gamma}\sum_{\langle ij\rangle\|\gamma}\Big\{\Big[-r_1\Big(\vec{S}_i\cdot\vec{S}_j+\frac{3}{4}\Big)+r_2\Big(\vec{S}_i\cdot\vec{S}_j-\frac{1}{4}\Big)\Big]\Big(\frac{1}{4}-\tau_i^{(\gamma)}\tau_j^{(\gamma)}\Big)$$
$$+(r_3+r_4)\Big(\vec{S}_i\cdot\vec{S}_j-\frac{1}{4}\Big)\Big(\tau_i^{(\gamma)}+\frac{1}{2}\Big)\Big(\tau_j^{(\gamma)}+\frac{1}{2}\Big)\Big\}+E_z\sum_i \tau_i^c.$$

KK model

Experimental observations:

K_2CuF_4 — the FM spin phase

$KCuF_3$ finite Hund's exchange η favors AO order stabilizing A-AF

$KCuF_3$ exhibits spinon excitations for $T > T_N$

In this regime behaves as the 1D quantum antiferromagnet

Spin-orbital entanglement near the QCP

Example: Kugel-Khomskii (KK) model (d^9)

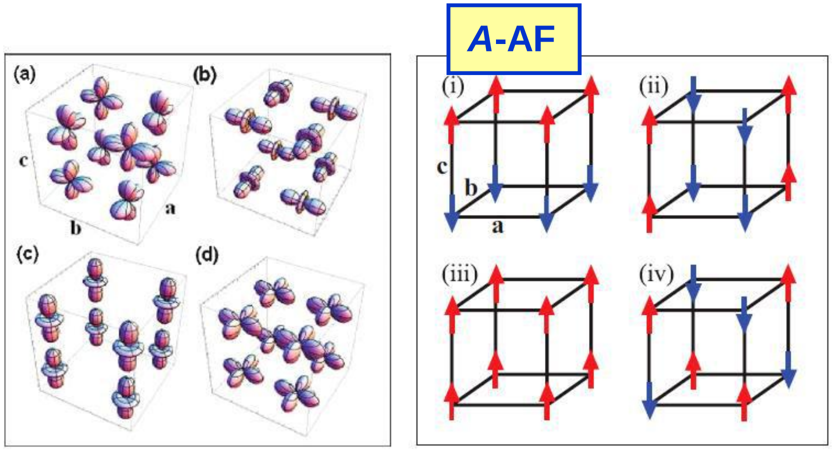

e_g **orbitals** T**=1/2** **spins** S**=1/2**

Parameters: (1) E_z/J – e_g orbital splitting
(2) J_H/U – Hund´s exchange

Quantum critical point: $(E_z,J_H) = (0,0)$

Entanglement#1: near the QCP

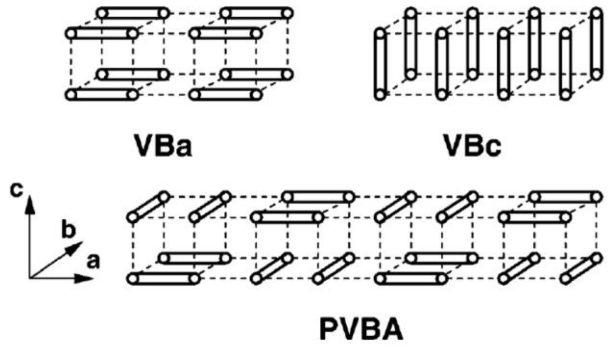

Spin disordered states

***A*-AF** phase in $KCuF_3$

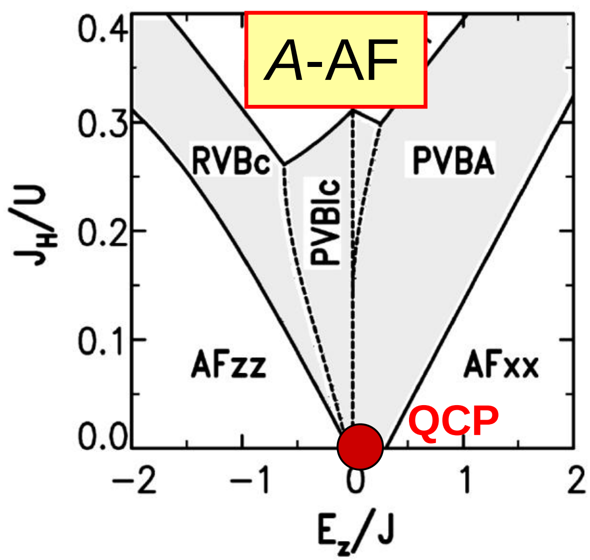

Phase diagram of the d^9 model

[L.F. Feiner, AMO, J. Zaanen, PRL **78**, 2799 (97)]

Orbital Hubbard model for e_g orbitals

Hamiltonian for e_g electrons couples two directional e_g-orbitals

Real basis:

$$H_t(e_g) = -t \sum_{\alpha} \sum_{\langle ij \rangle \| \alpha, \sigma} a^\dagger_{i\zeta_\alpha\sigma} a_{j\zeta_\alpha\sigma}$$

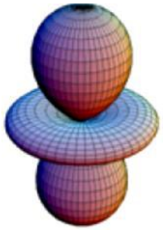

$$|z\rangle \equiv \frac{1}{\sqrt{6}}(3z^2 - r^2), \qquad |\bar{z}\rangle \equiv \frac{1}{\sqrt{2}}(x^2 - y^2)$$

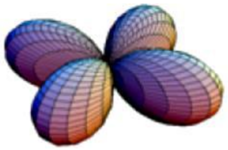

$$H_t^\uparrow(e_g) = -\frac{1}{4} t \sum_{\langle ij \rangle \| ab} \left[3a^\dagger_{i\bar{z}} a_{j\bar{z}} + a^\dagger_{iz} a_{jz} \mp \sqrt{3} \left(a^\dagger_{i\bar{z}} a_{jz} + a^\dagger_{iz} a_{j\bar{z}} \right) \right] - t \sum_{\langle ij \rangle \| c} a^\dagger_{iz} a_{jz}$$

complex e_g orbitals

$$|j+\rangle = \frac{1}{\sqrt{2}}(|jz\rangle - i|j\bar{z}\rangle), \qquad |j-\rangle = \frac{1}{\sqrt{2}}(|jz\rangle + i|j\bar{z}\rangle)$$

$$\mathcal{H}^\uparrow(e_g) = -\frac{1}{2} t \sum_{\alpha} \sum_{\langle ij \rangle \| \alpha} \left[\left(a^\dagger_{i+} a_{j+} + a^\dagger_{i-} a_{j-} \right) + \gamma \left(e^{-i\chi_\alpha} a^\dagger_{i+} a_{j-} + e^{+i\chi_\alpha} a^\dagger_{i-} a_{j+} \right) \right]$$

with $\chi_a = +2\pi/3$, $\chi_b = -2\pi/3$, and $\chi_c = 0$ has cubic symmetry

with interaction $\bar{U} \sum_i n_{i+} n_{i-}$ => ***orbital Hubbard model***

Phase diagram: 2D Kugel-Khomskii model

Entanglement #2: in 2D model

the $(E_z/J, \eta)$ plane

ortho-AF phase

$\eta = J_H/U$

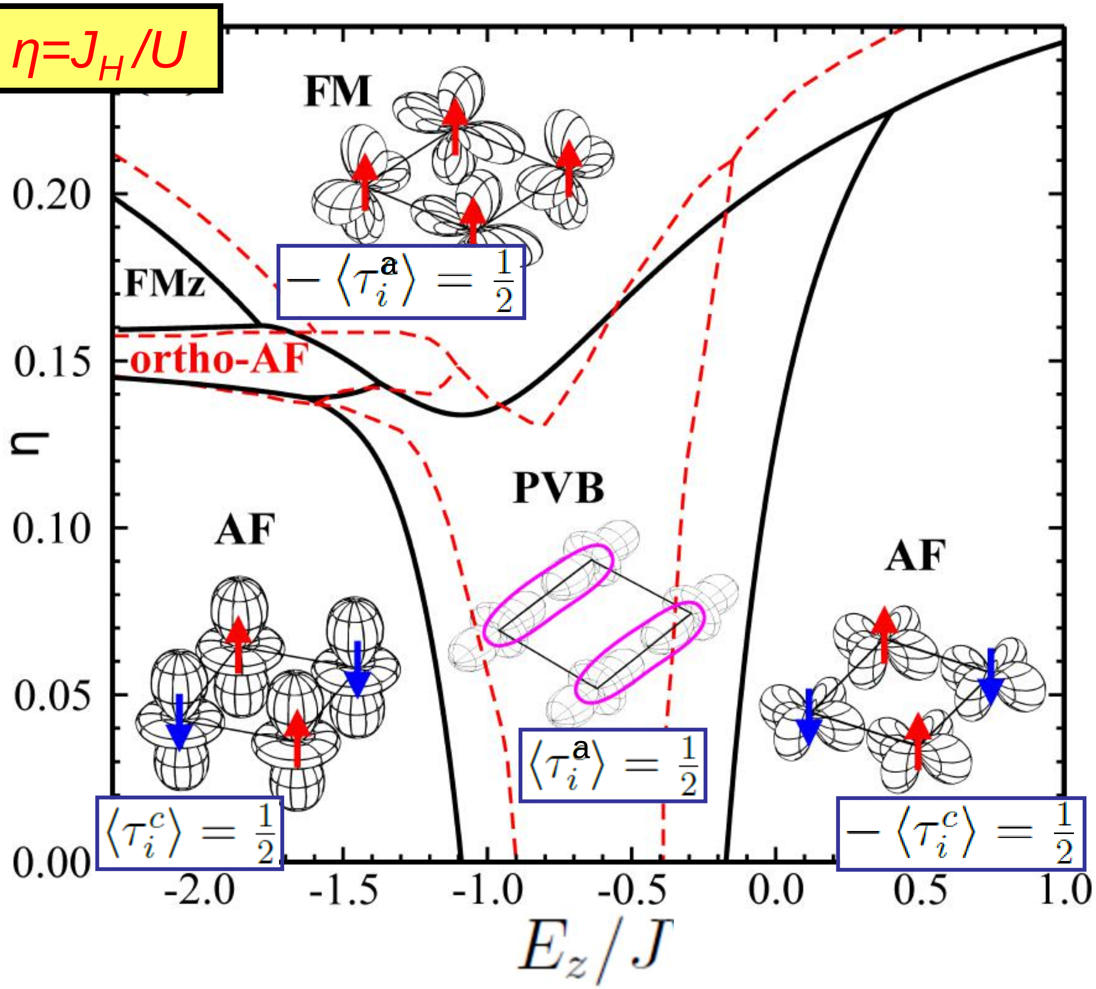

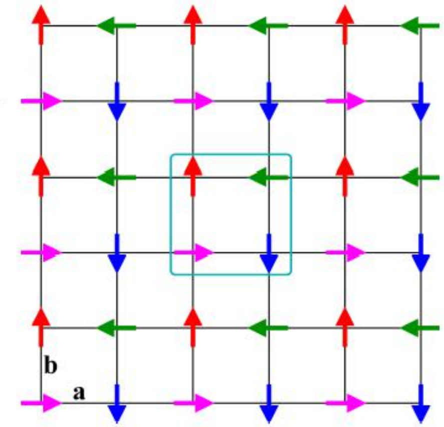

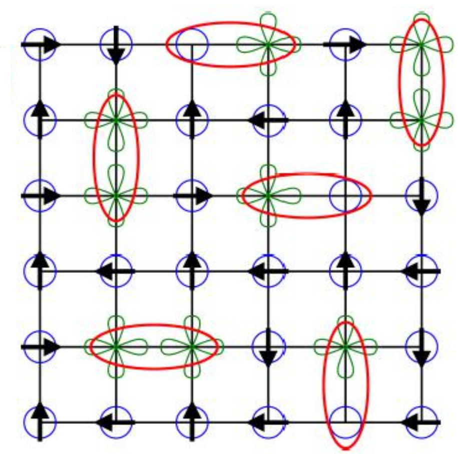

orbital excitations $|z\rangle \rightarrow |\bar{z}\rangle$

Much weaker AF interactions between holes in $|z\rangle$ orbitals than in $|\bar{z}\rangle$

a quantum critical point $Q_{2D} = (-0.5, 0)$ in the $(E_z/J, \eta)$ plane

Entanglement: spin excitations in the FM phase

$$\boxed{\omega_{\vec{k}}^{(0)} = I^{(0)} + P^{(0)}(\vec{k}) = 4J_{\Diamond}S\,(1-\gamma_{\vec{k}})}$$

Variational Approximation (VA)

$J_{\Diamond} \to J_{\blacklozenge}$, and the magnon dispersion would soften.

for each value of momentum k independently.

$$\boxed{\omega_{\vec{k}}(\{\theta_{iL}\}) = I(\{\theta_{iL}\};\vec{k}) + P(\{\theta_{iL}\};\vec{k})}$$

the angles $\{\theta_{iL}\}$ are real and $L = A, B$ refers to the sublattice

the constraint $\theta_i \equiv \theta_{iA} = \theta_{iB}$

defines the Simplified Variational Approximation (SVA)

exact diagonalization employing a Numerical *Ansatz* (NA)

with six states per sublattice:

Entanglement: orbital background and its modification

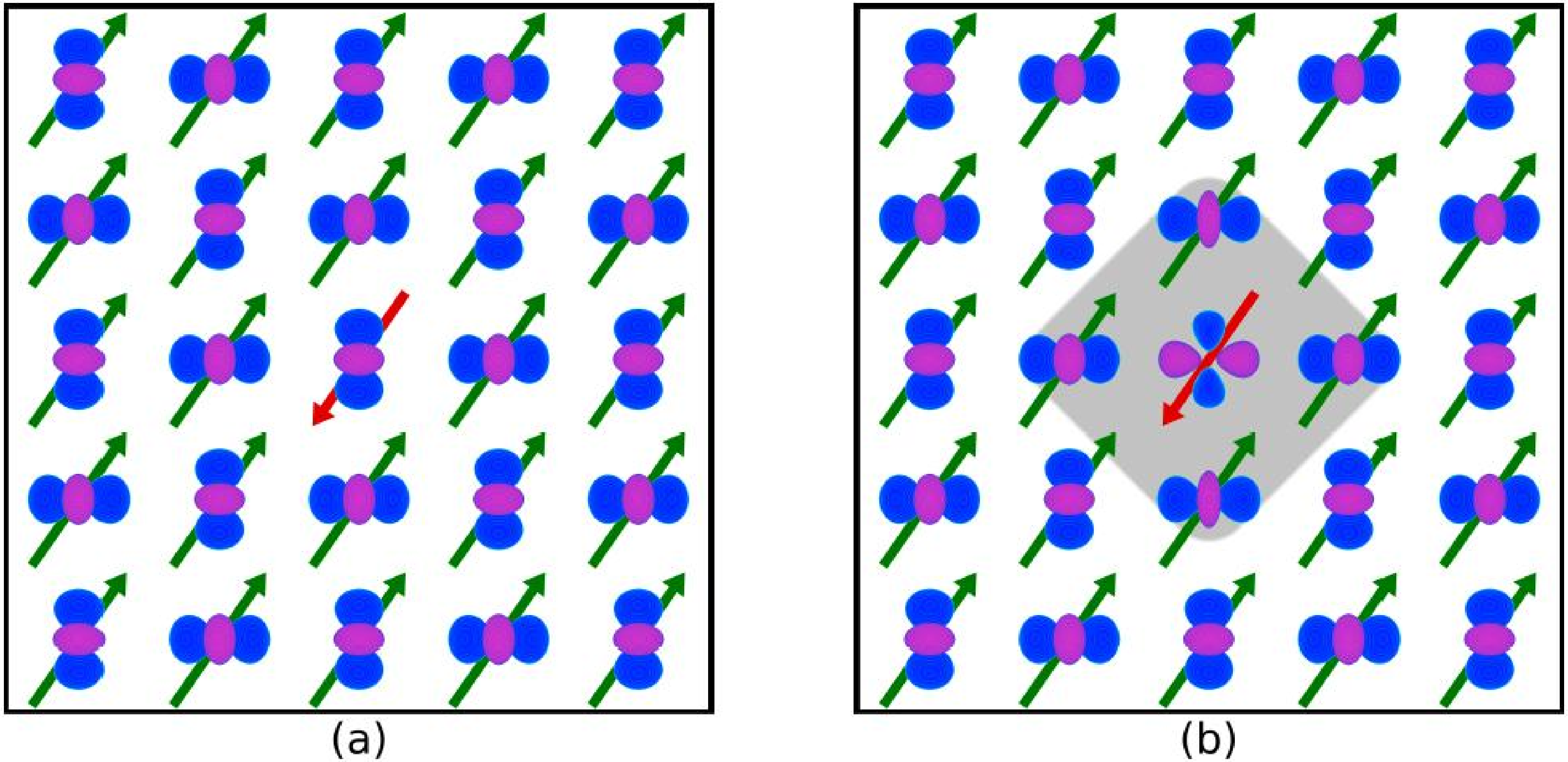

Fig. 11: *Artist's view of a spin excitation (inverted red arrow at the central site) in the FM plane of K_2CuF_4 (green arrows) and AO order of the orbitals occupied by holes at $E_z = -0.8J$, with: (a) frozen orbitals; (b) optimized orbitals at the central site and at four its neighboring sites in the square lattice, forming a quasiparticle (dressed magnon). The above value of E_z leads to the expected AO order in K_2CuF_4, with $\theta_{opt} \simeq 71°$ in Eqs. (14). When the VA is used, case (a) is still realized at $\vec{k} \simeq 0$, while case (b) represents a dressed magnon with $\vec{k} \simeq M$ where orbital states in the shaded cluster are radically different from those shown for frozen orbitals in (a).*

Entanglement #3: Modified FM magnons

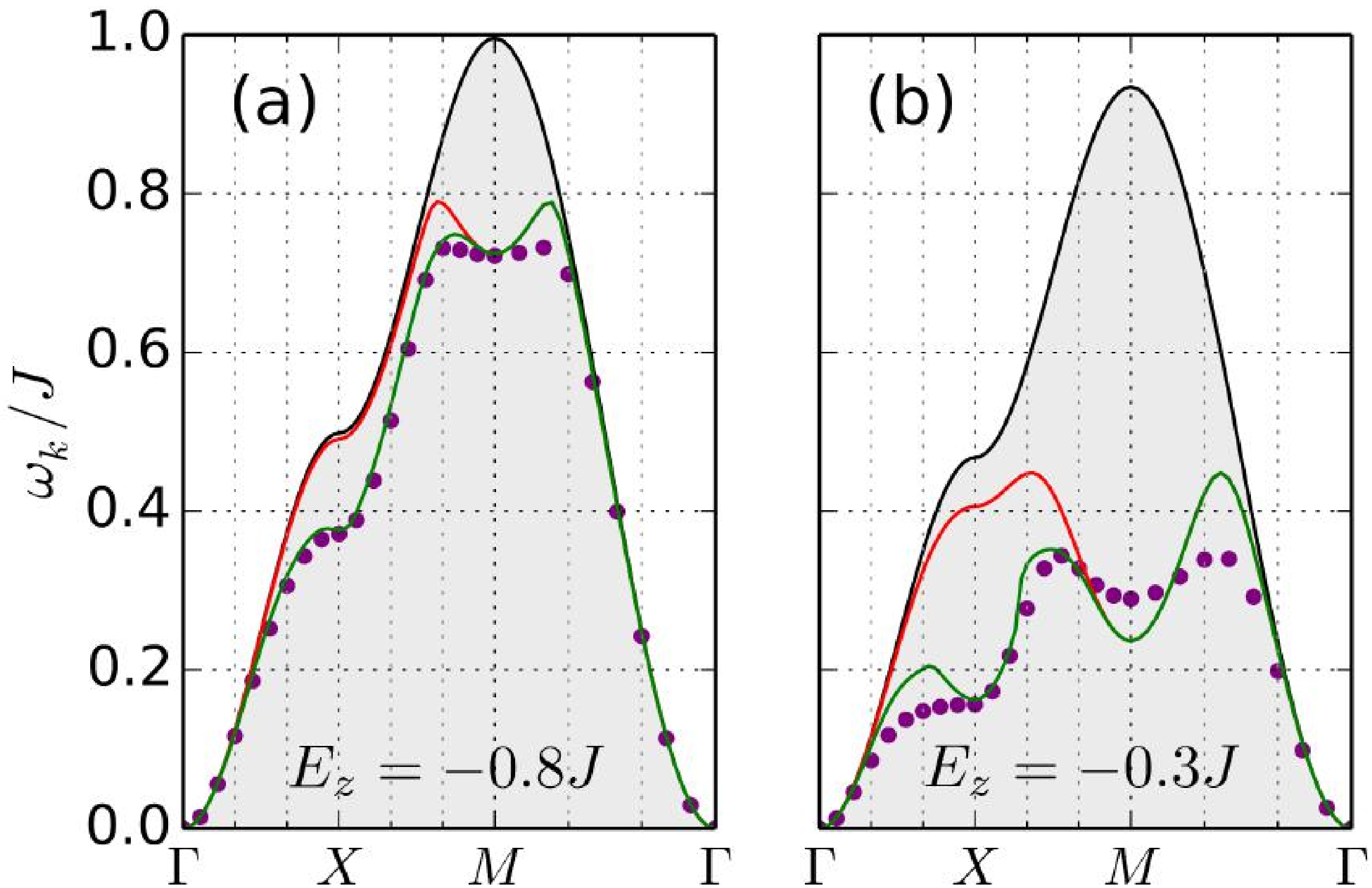

Fig. 12: *The magnon energy $\omega_{\vec{k}}/J$ obtained for the FM state of K_2CuF_4 at $J_H/U = 0.2$ and: (a) $E_z = -0.80J$ and (b) $E_z = -0.30J$. Results are presented for four approximations: frozen orbitals (black line and grey background), the VA (green line), the SVA (red line), and the 12-state NA (purple dots). The high symmetry points are: $\Gamma = (0,0)$, $X = (\pi, 0)$, $M = (\pi, \pi)$.*

Weak entanglement: $LaMnO_3$

$$\mathcal{H}_e = \frac{1}{16}\sum_{\gamma}\sum_{\langle ij\rangle\parallel\gamma}\left\{-\frac{8}{5}\frac{t^2}{\varepsilon(^6A_1)}\left(\vec{S}_i\cdot\vec{S}_j+6\right)\mathcal{P}^{(\gamma)}_{\langle ij\rangle}+\left[\frac{t^2}{\varepsilon(^4E)}+\frac{3}{5}\frac{t^2}{\varepsilon(^4A_1)}\right]\left(\vec{S}_i\cdot\vec{S}_j-4\right)\mathcal{P}^{(\gamma)}_{\langle ij\rangle}\right.$$
$$\left.+\left[\frac{t^2}{\varepsilon(^4E)}+\frac{t^2}{\varepsilon(^4A_2)}\right]\left(\vec{S}_i\cdot\vec{S}_j-4\right)\mathcal{Q}^{(\gamma)}_{\langle ij\rangle}\right\}+E_z\sum_i\tau_i^c. \quad (49)$$

$$\mathcal{H}_t = \frac{1}{8}J\beta r_t\left(\vec{S}_i\cdot\vec{S}_j-4\right)$$

$$\beta \simeq \frac{1}{9}$$

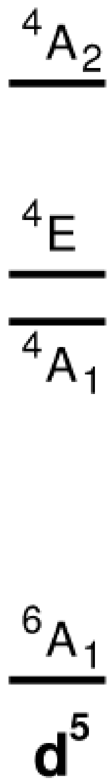

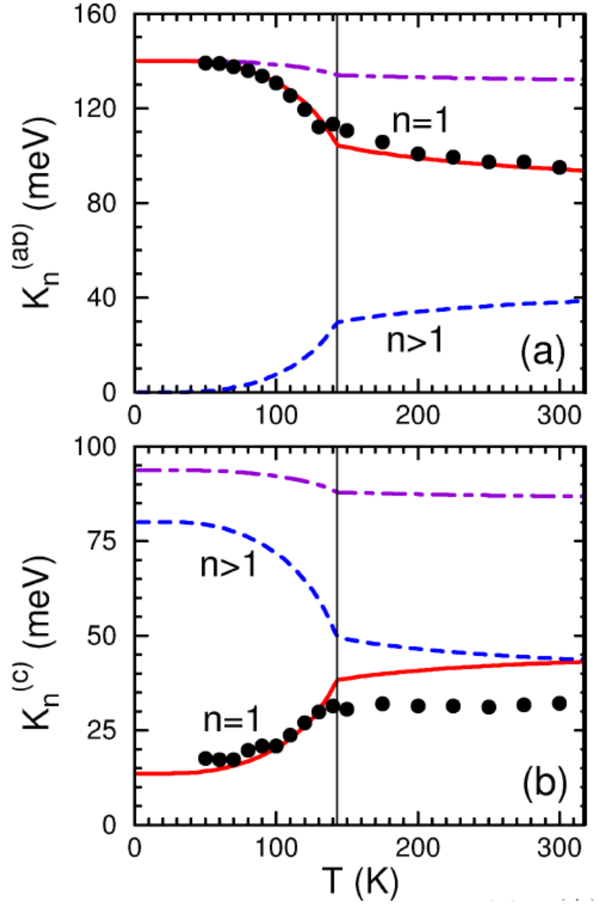

Kinetic energies per bond $K_n^{(\gamma)}$

Here the optical spectra weights are reproduced by disentangled spin-orbital superexchange

Spin-orbital superexchange in RVO_3

In t_{2g} **systems** (***d*¹**,***d*²**) two states are active, e.g. *yz* i *zx* for the axis *c* – they are described by **quantum** operators:

$$\vec{T}_i = \{T_i^x, T_i^y, T_i^z\}$$

$$T_i^x = \tfrac{1}{2}\sigma_i^x,\; T_i^y = \tfrac{1}{2}\sigma_i^y,\; T_i^z = \tfrac{1}{2}\sigma_i^z.$$

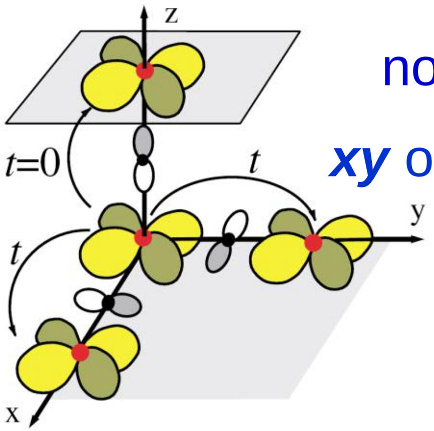

no hopping ||*c*

xy orbital is called ***c***

[A.B. Harris *et al*., PRL **91**, 087206 (03)]

Scalar product $\vec{T}_i \cdot \vec{T}_j$ but for *η*>0 also:

$$\vec{T}_i \otimes \vec{T}_j \equiv T_i^x T_j^x - T_i^y T_j^y + T_i^z T_j^z$$

Orbital interactions have cubic symmetry

Orbital SU(2) symmetry is broken !

$$|a\rangle \equiv |yz\rangle, \qquad |b\rangle \equiv |zx\rangle, \qquad |c\rangle \equiv |xy\rangle.$$

Spin-orbit superexchange in RVO_3 ***d*** ² (*S* = 1):

$$\mathcal{H}_0 = \frac{1}{2}J \sum_{\langle ij\rangle \parallel \gamma} (\vec{S}_i \cdot \vec{S}_j + 1)\left(\vec{\tau}_i \cdot \vec{\tau}_j + \frac{1}{4}n_i n_j\right)^{(\gamma)}$$

Entanglement expected !

Optical spectra: HS (n=1) and LS (n=2,3) weights

charge excitations ε_n arising from the transitions to [see Fig. 6(b)]:

(i) a high-spin state $^4A_2$ at energy $U-3J_H$,

(ii) two degenerate low-spin states $^2T_1$ and ^2E at U, and

(iii) a $^2T_2$ low-spin state at $U+2J_H$ [16].

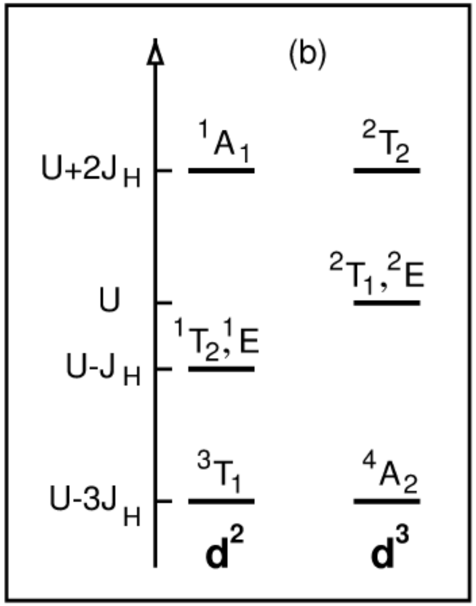

Energies of charge excitations ε_n

One derives a HS contribution $H_1^{(c)}(ij)$ and $H_1^{(ab)}(ij)$

$\frac{1}{3}(\vec{S}_i\cdot\vec{S}_j+2)$ is the projection operator on the HS state for $S=1$ spins

$$
\begin{aligned}
H_1^{(c)}(ij) &= -\tfrac{1}{3}Jr_1(\vec{S}_i\cdot\vec{S}_j+2)\left(\tfrac{1}{4}-\vec{\tau}_i\cdot\vec{\tau}_j\right),\\
H_1^{(ab)}(ij) &= -\tfrac{1}{6}Jr_1(\vec{S}_i\cdot\vec{S}_j+2)\left(\tfrac{1}{4}-\tau_i^z\tau_j^z\right).
\end{aligned}
$$

LS excitations ($n=2,3$) contain instead the spin operator $(1-\vec{S}_i\cdot\vec{S}_j)$

$$
\begin{aligned}
H_2^{(c)}(ij) &= -\tfrac{1}{12}\,J\,(1-\vec{S}_i\cdot\vec{S}_j)\left(\tfrac{7}{4}-\tau_i^z\tau_j^z-\tau_i^x\tau_j^x+5\tau_i^y\tau_j^y\right),\\
H_3^{(c)}(ij) &= -\tfrac{1}{4}Jr_5(1-\vec{S}_i\cdot\vec{S}_j)\left(\tfrac{1}{4}+\tau_i^z\tau_j^z+\tau_i^x\tau_j^x-\tau_i^y\tau_j^y\right).
\end{aligned}
$$

$$
\begin{aligned}
H_2^{(ab)}(ij) &= -\tfrac{1}{8}\,J\,(1-\vec{S}_i\cdot\vec{S}_j)\left(\tfrac{19}{12}\mp\tfrac{1}{2}\tau_i^z\mp\tfrac{1}{2}\tau_j^z-\tfrac{1}{3}\tau_i^z\tau_j^z\right),\\
H_3^{(ab)}(ij) &= -\tfrac{1}{8}Jr_5(1-\vec{S}_i\cdot\vec{S}_j)\left(\tfrac{5}{4}\mp\tfrac{1}{2}\tau_i^z\mp\tfrac{1}{2}\tau_j^z+\tau_i^z\tau_j^z\right),
\end{aligned}
$$

Spin-orbital order in a t_{2g} system

$$
\begin{aligned}
J_c &= \tfrac{1}{2}J\left\{\eta r_1 - (r_1 - \eta r_1 - \eta r_5)\left(\tfrac{1}{4} + \langle \vec{\tau}_i \cdot \vec{\tau}_j \rangle\right) - 2\eta r_5 \langle \tau_i^y \tau_j^y \rangle\right\}, \\
J_{ab} &= \tfrac{1}{4}J\left\{1 - \eta r_1 - \eta r_5 + (r_1 - \eta r_1 - \eta r_5)\left(\tfrac{1}{4} + \langle \tau_i^z \tau_j^z \rangle\right)\right\},
\end{aligned}
$$

In the orbital sector one finds at the same time,

$$
\begin{aligned}
H_\tau &= \sum_{\langle ij\rangle_c} \left[J_c^\tau \vec{\tau}_i \cdot \vec{\tau}_j - J(1 - s_c)\eta r_5 \tau_i^y \tau_j^y\right] + J_{ab}^\tau \sum_{\langle ij\rangle_{ab}} \tau_i^z \tau_j^z, \\
J_c^\tau &= \tfrac{1}{2}J\left[(1 + s_c)r_1 + (1 - s_c)\eta(r_1 + r_5)\right], \\
J_{ab}^\tau &= \tfrac{1}{4}J\left[(1 - s_{ab})r_1 + (1 + s_{ab})\eta(r_1 + r_5)\right],
\end{aligned}
$$

depending on spin correlations: $s_c = \langle \vec{S}_i \cdot \vec{S}_j \rangle_c$ and $s_{ab} = -\langle \vec{S}_i \cdot \vec{S}_j \rangle_{ab}$.

$$
\boxed{H_\tau^{(0)} = J r_1 \left[\sum_{\langle ij\rangle_c} \vec{\tau}_i \cdot \vec{\tau}_j + \frac{1}{2}\eta\left(1 + \frac{r_5}{r_1}\right) \sum_{\langle ij\rangle_{ab}} \tau_i^z \tau_j^z\right]}
$$

Entanglement #4: **Optical spectral weights for $LaVO_3$ (*C*-AF)**

mean-field approach fails:

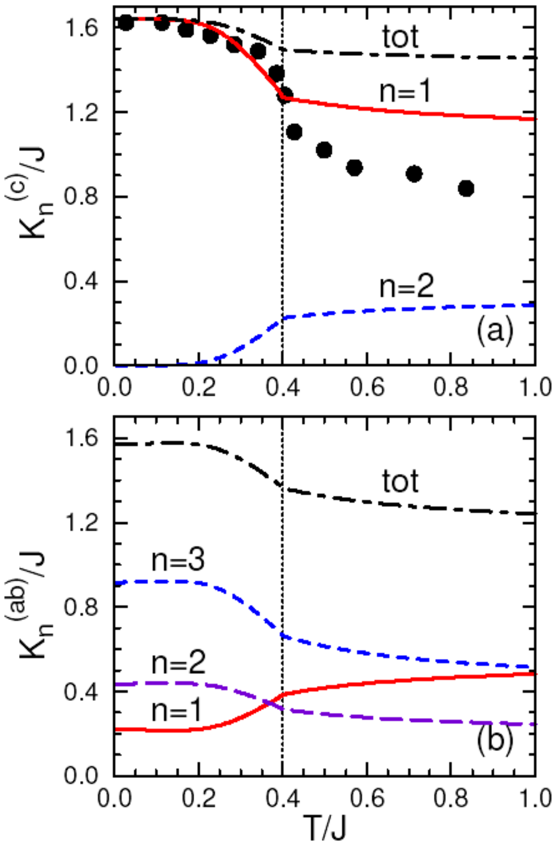

Data: S. Miyasaka et al.,

[JPSJ **71**, 2086 (2002)]

orbital and spin-orbital dynamics

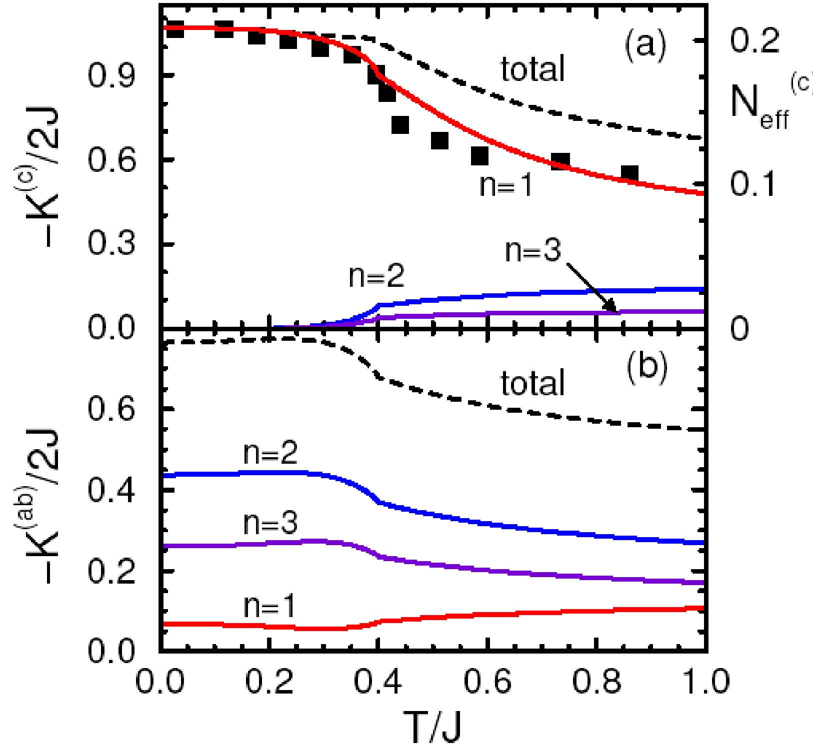

weak orbital order unlike in $LaMnO_3$

spin-orbital entanglement is crucial at *T*>0!

[G. Khaliullin, P. Horsch, and AMO, PRB **70**, 195103 (04)]

SOE 18 Sep

(Note: no entanglement in $LaMnO_3$)

Phase Diagram of RVO_3 (R =Lu,…,La)

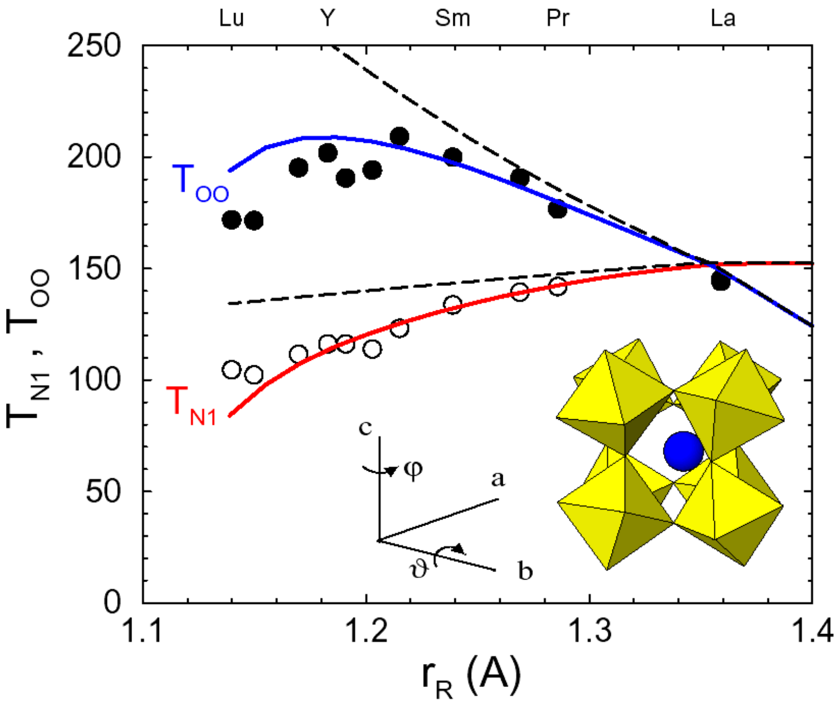

FIG. 1: (color) The orbital transition T_{OO} and Néel T_{N1}

with superexchange:

$\boxed{J = 200\ \mathrm{K}}$

C-AF phase

G-AF phase

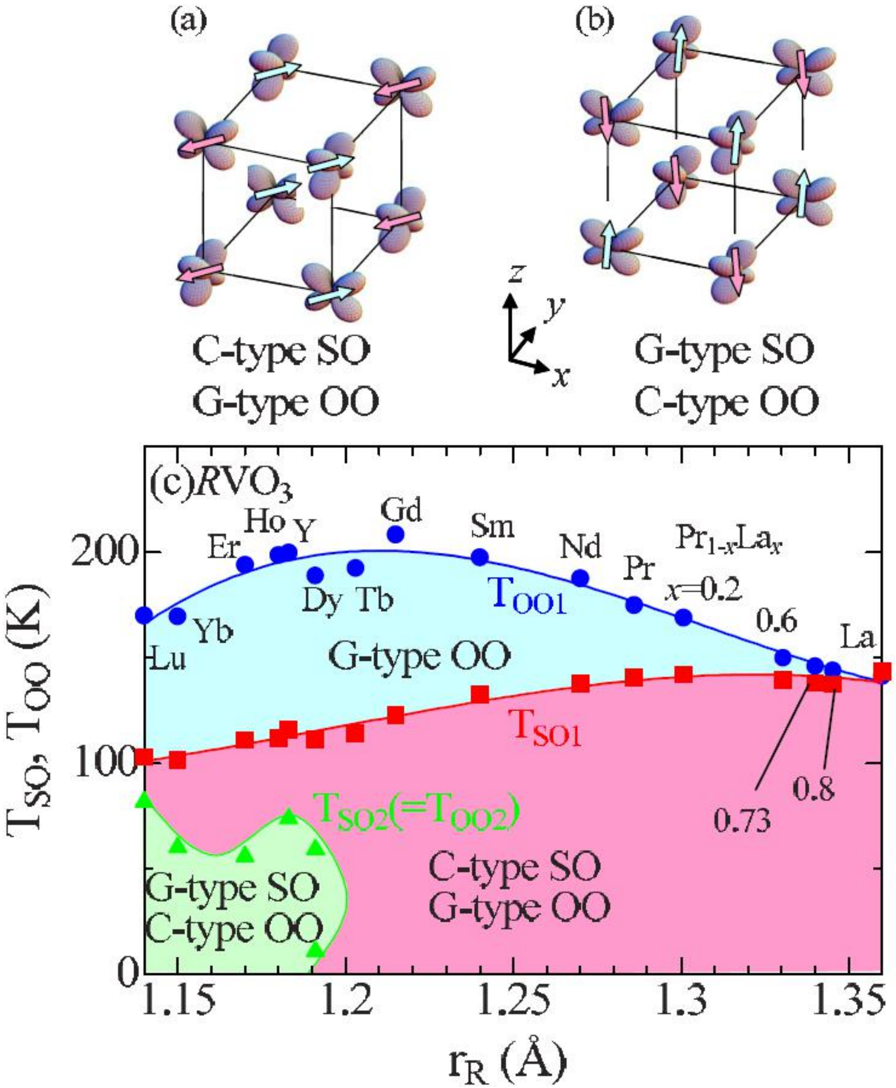

[P. Horsch *et al*., PRL **100**, 167205 (2008)]

[J. Fujioka *et al*., PRB **82**, 144425 (2008)]

Entanglement #5: **Phase Diagram of RVO_3 (R =Lu,…,La)**

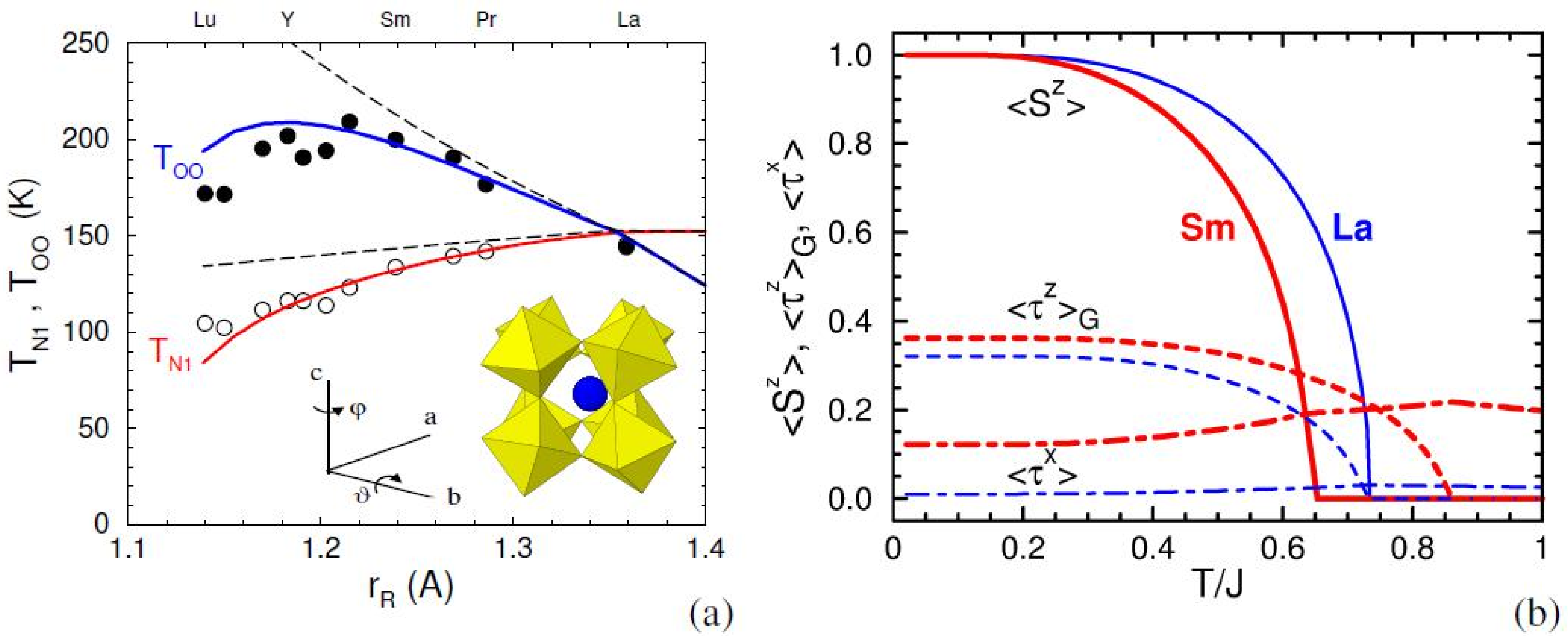

Fig. 14: *Phase transitions in the vanadium perovskites RVO_3: (a) phase diagram with the orbital T_{OO} and Néel T_{N1} transition temperatures obtained from the theory with and without orbital-lattice coupling (solid and dashed lines) [50], and from experiment (circles) [51]; (b) spin $\langle S_i^z \rangle$ (solid) and G-type orbital $\langle \tau_i^z \rangle_G$ (dashed) order parameters, vanishing at T_{N1} and T_{OO}, respectively, and the transverse orbital polarization $\langle \tau_i^x \rangle$ (dashed-dotted lines) for $LaVO_3$ and $SmVO_3$ (thin and heavy lines). Images reproduced from Ref. [50].*

T_{N1} modified due to s-o entanglement !

IOP PUBLISHING JOURNAL OF PHYSICS: CONDENSED MATTER

J. Phys.: Condens. Matter **24** (2012) 313201 (28pp) doi:10.1088/0953-8984/24/31/313201

TOPICAL REVIEW

Fingerprints of spin–orbital entanglement in transition metal oxides

Andrzej M Oleś

Contents

1. Introduction: entanglement in many-body systems 2
2. Orbital and spin–orbital superexchange 3
   2.1. Intrinsic frustration of orbital interactions 3
   2.2. Spin–orbital superexchange models 5
3. Spin–orbital entanglement 7
   3.1. Exact versus mean field states for a bond 7
   3.2. Entanglement in the $SU(2)\otimes SU(2)$ spin–orbital model 8
   3.3. Entanglement in t_{2g} spin–orbital models 10
4. Entangled states in the RVO_3 perovskites 12
   4.1. Optical spectral weights for $LaVO_3$ 12
   4.2. Phase diagram of the RVO_3 perovskites 13
   4.3. Peierls dimerization in YVO_3 15
5. Entanglement in the ground states of spin–orbital models 17
   5.1. The Kugel–Khomskii model 17
   5.2. Spin–orbital resonating valence bond liquid 19
6. Hole propagation in a Mott insulator with coupled spin–orbital order 23
7. Discussion and summary 25

Entanglement in the triangular lattice

$$S_{ij} \equiv \frac{1}{d} \sum_n \langle n|\vec{S}_i \cdot \vec{S}_j|n\rangle \,, \tag{54}$$
$$T_{ij} \equiv \frac{1}{d} \sum_n \langle n|(\vec{T}_i \cdot \vec{T}_j)^{(\gamma)}|n\rangle \,, \tag{55}$$
$$\begin{aligned} C_{ij} &\equiv \frac{1}{d} \sum_n \langle n|(\vec{S}_i \cdot \vec{S}_j - S_{ij})\,(\vec{T}_i \cdot \vec{T}_j - T_{ij})^{(\gamma)}|n\rangle \\ &= \frac{1}{d} \sum_n \langle n|(\vec{S}_i \cdot \vec{S}_j)(\vec{T}_i \cdot \vec{T}_j)^{(\gamma)}|n\rangle - \Big(\frac{1}{d} \sum_n \langle n|\vec{S}_i \cdot \vec{S}_j|n\rangle\Big)\Big(\frac{1}{d} \sum_m \langle m|(\vec{T}_i \cdot \vec{T}_j)^{(\gamma)}|m\rangle\Big), \end{aligned} \tag{56}$$

The effective spin-orbital model considered here for $NaTiO_2$ reads [54],

$$\mathcal{H} = J\left((1-\alpha)\,\mathcal{H}_s + \sqrt{(1-\alpha)\alpha}\,\mathcal{H}_m + \alpha\,\mathcal{H}_d\right).$$

The parameter α in Eq. (57) is given by the hopping elements as follows,

$$\alpha = (t')^2 / \left[t^2 + (t')^2\right] \,,$$

interpolates between the superexchange $\mathcal{H}_s\,(\alpha = 0)$ and kinetic exchange $\mathcal{H}_d\,(\alpha = 1)$

Entanglement #6: Triangular lattice

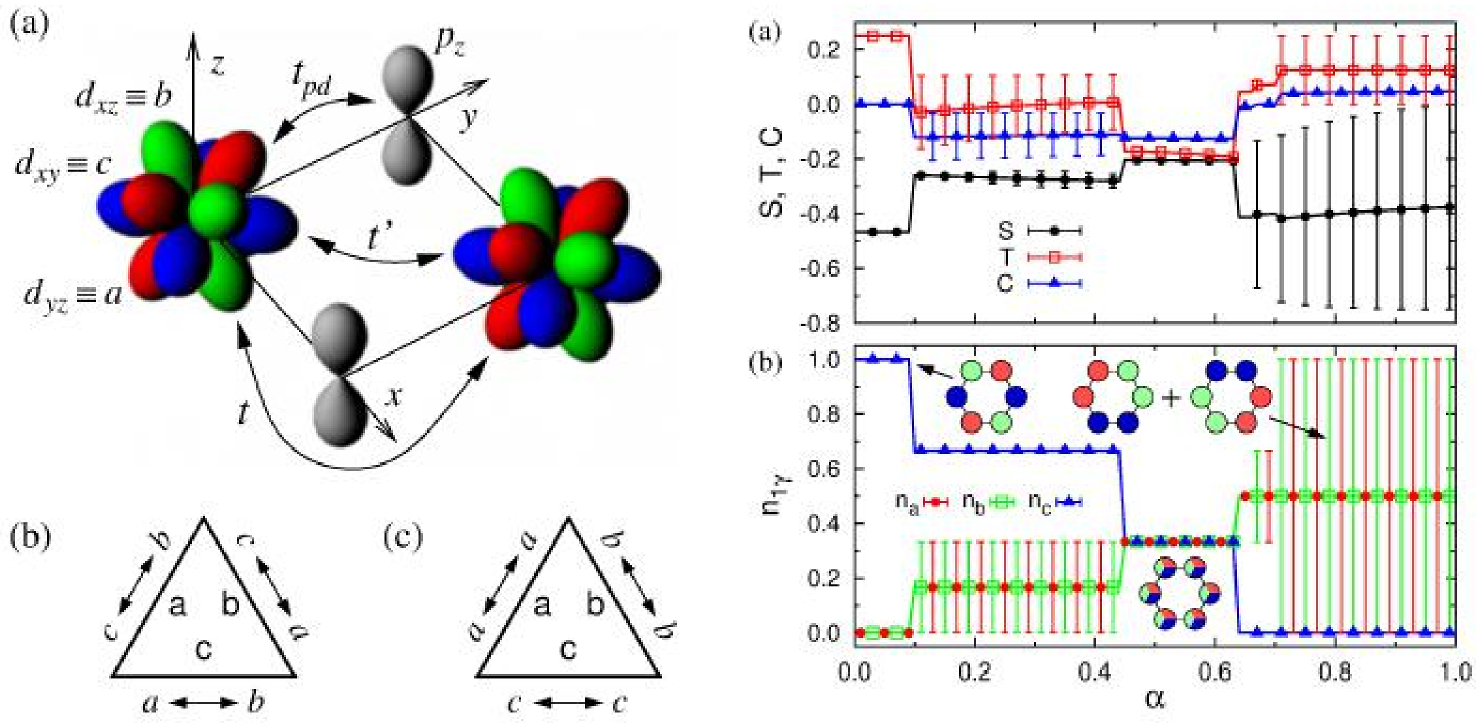

Fig. 15: *Left — (a) Hopping processes between t_{2g} orbitals along a bond parallel to the c axis in NaTiO$_2$: (i) t_{pd} between Ti(t_{2g}) and O($2p_z$) orbitals—two t_{pd} transitions define an effective hopping t, and (ii) direct d-d hopping t'. The t_{2g} orbitals (7) are shown by different color. The bottom part gives the hopping processes along the $\gamma = a, b, c$ axes that contribute to Eq. (57): (b) superexchange and (c) direct exchange. Right — Ground state for a free hexagon as a function of α: (a) bond correlations—spin S_{ij} Eq. (54) (circles), orbital T_{ij} Eq. (55) (squares), and spin–orbital C_{ij} Eq. (56) (triangles); (b) orbital electron densities $n_{1\gamma}$ at a representative site $i = 1$ (left-most site): n_{1a} (circles), n_{1b} (squares), n_{1c} (triangles). The insets indicate the orbital configurations favored by the superexchange ($\alpha = 0$), by mixed interactions $0.44 < \alpha < 0.63$, and by the direct exchange ($\alpha = 1$). The vertical lines indicate an exact range of configurations*

Maximal frustration: No order in the Kitaev model

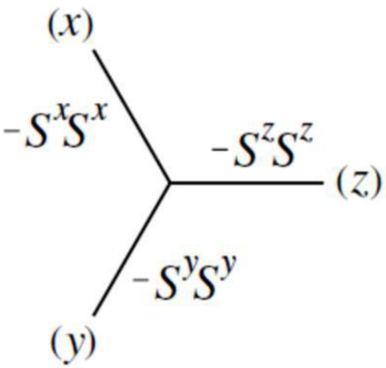

The Kitaev Hamiltonian is (with FM exchange)

$$H = -J_x \sum_{\langle ij \rangle_x} \sigma_i^x \sigma_j^x - J_y \sum_{\langle ij \rangle_y} \sigma_i^y \sigma_j^y - J_z \sum_{\langle ij \rangle_z} \sigma_i^z \sigma_j^z,$$

[A. Kitaev, Ann. Phys. **321**, 2 (2006)]

[G. Baskaran *et al*., PRL **98**, 247201 (2007)]

Two-spin correlations vanish beyond NN pairs

Gapless but short range spin liquid

A model for topological quantum computations

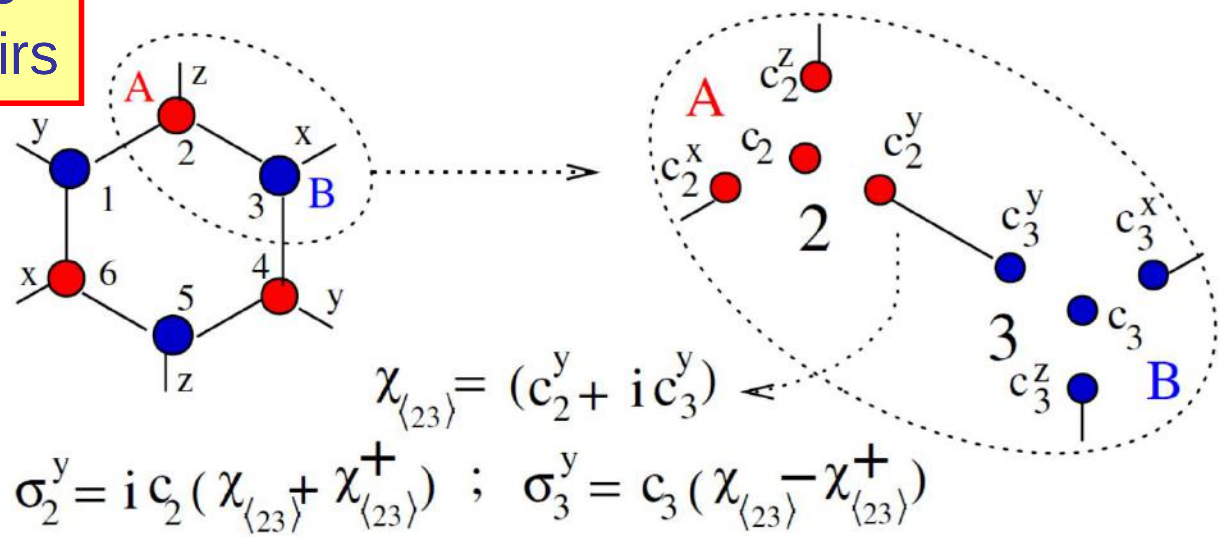

FIG. 1 (color online). Elementary hexagon and "bond fermion" construction. A spin is replaced with 4 Majorana fermions (c, c^x, c^y, c^z). Bond fermion $\chi_{\langle 23 \rangle}$ and spin operator are defined. *A* and *B* denote the sublattice index.

Entanglement #7: Kitaev-Heisenberg model

$$\mathcal{H}_{HK} = J \sum_{\langle ij \rangle} \left(\vec{S}_i \cdot \vec{S}_j \right) + K \sum_{\gamma \| \langle ij \rangle} S_i^\gamma S_j^\gamma ,$$

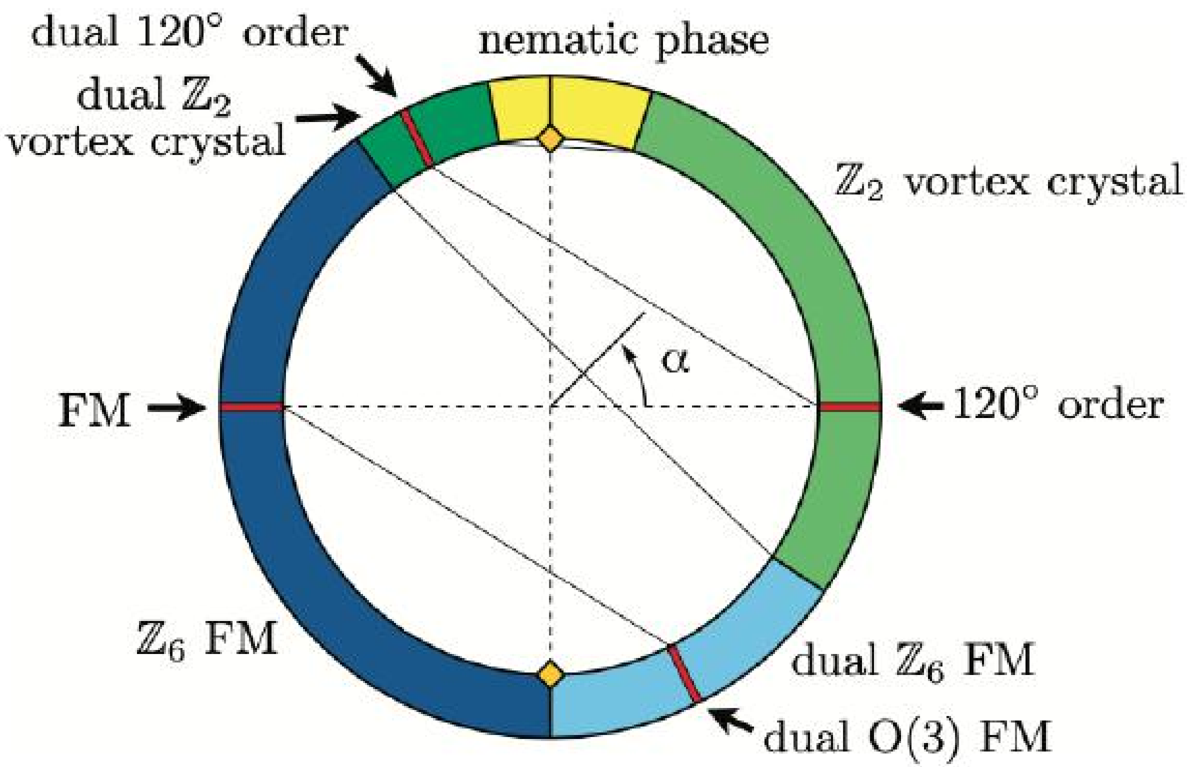

Fig. 16: *Phase diagram of the Kitaev-Heisenberg model Eq.* (59) *with parametrization* $(J, K) = (\cos\alpha, \sin\alpha)$ *as obtained from exact diagonalization data. Solid lines show the mapping between two Klein-dual points. Red lines mark the location of the four SU(2)—symmetric points. Yellow diamonds mark the two Kitaev points. Image reproduced from Ref. [56].*

one-dimensional (1D) Kugel-Khomskii Hamiltonian

the one-dimensional (1D) Kugel-Khomskii Hamiltonian [14]:

$$\mathcal{H} = 4J \sum_{\langle ij \rangle} \left(\mathbf{S}_i \cdot \mathbf{S}_j + \frac{1}{4} \right) \left(\mathbf{T}_i \cdot \mathbf{T}_j + \frac{1}{4} \right) + E_z \sum_i T_i^z.$$

SU(4) limit: fractionalization and entanglement.

AF $\times$ AO correlations described by SU(4) singlets

a strong crystal field ($E_z \geqslant E_z^{cr}$), electrons occupy only lower-lying orbitals and show AF correlations (AF $\times$ FO)

[C.C. Chen *et al*., PRB **91**, 165102 (15)]

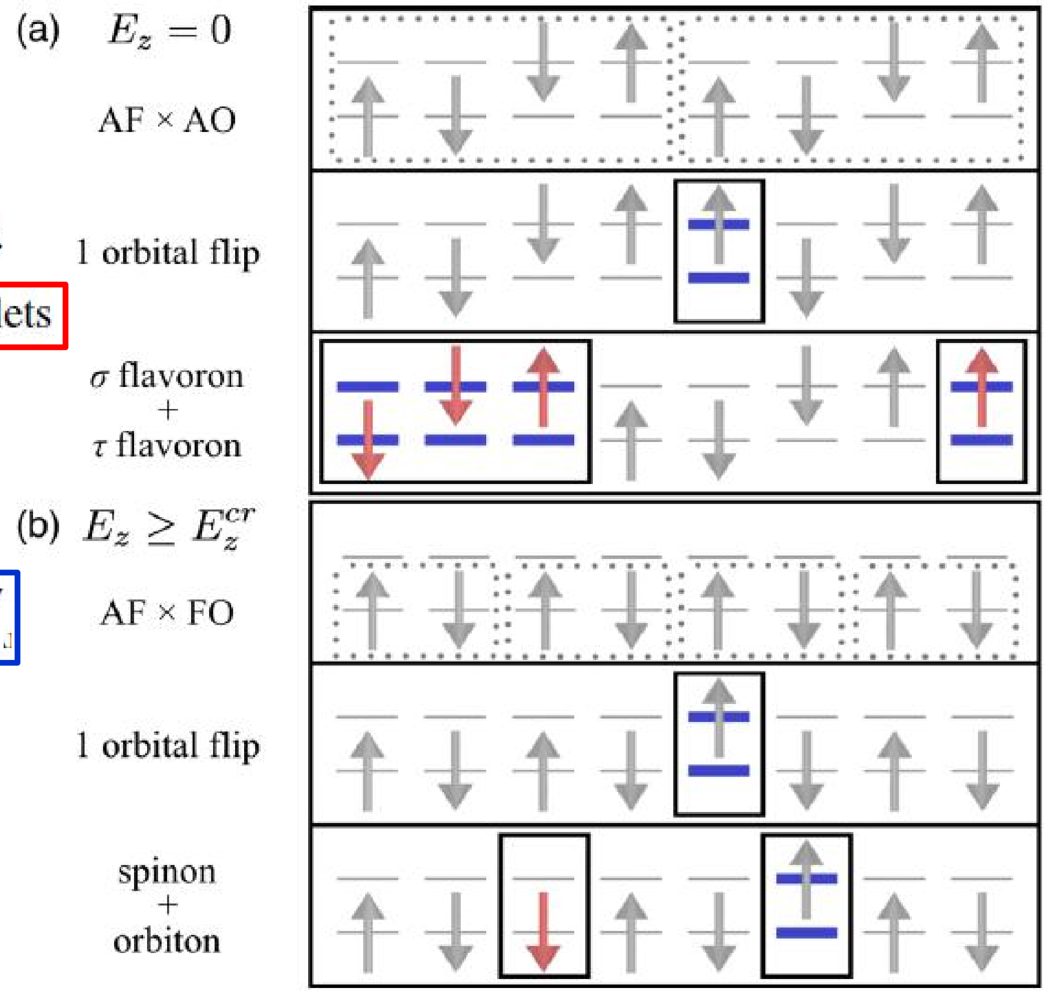

FIG. 2. (Color online) Illustrations showing collective excitations in the spin-orbital chain in two different limits described in the literature [20,29]: (a) without crystal field ($E_z = 0$), the ground-state exhibits AF $\times$ AO correlations described by SU(4) singlets (top row,

SOE 18 Sep

Canonical Orbital System $KCuF_3$

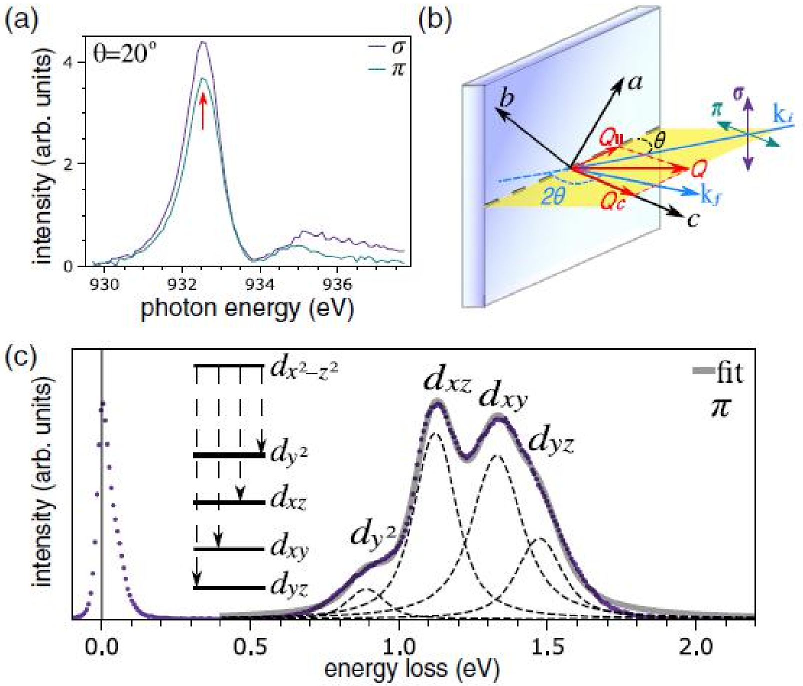

FIG. 1. Scattering geometry and overview of RIXS spectra.

the OO is mostly driven by the JT mechanism

Conclusion.—In summary, we performed high-resolution RIXS experiments on the orbitally ordered $KCuF_3$. The high-energy excitations are found to stem from localized *dd* orbital excitations, consistent with the *ab initio* calculation based on a single cluster.

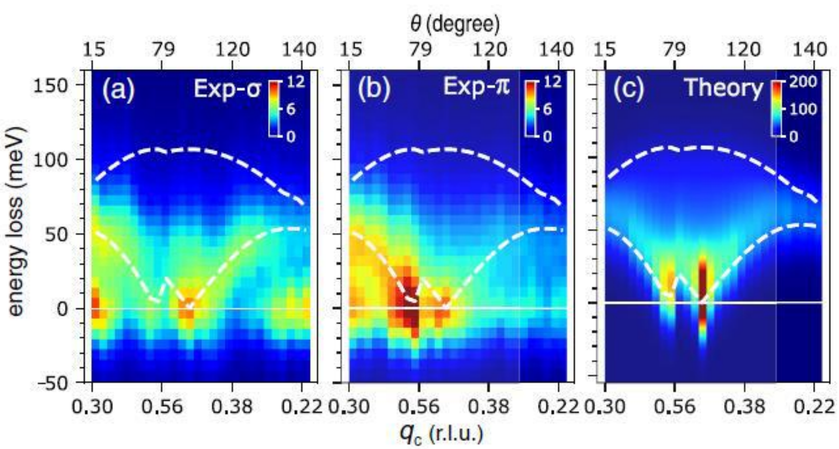

FIG. 4. Low-energy excitations of $KCuF_3$ revealed by the Cu L_3 edge

[J. Li *et al.*, PRL **126**, 165102 (21)]

Orbital Control of Effective Dimensionality:

[V. Bisogni *et al*., PRL **114**, 165102 (15)]

In the energy region between 1.5–2.6 eV, we observe orbital excitations, corresponding to the hole [9] in the $3d_{x^2-y^2}$ ground state being excited into a different orbital.

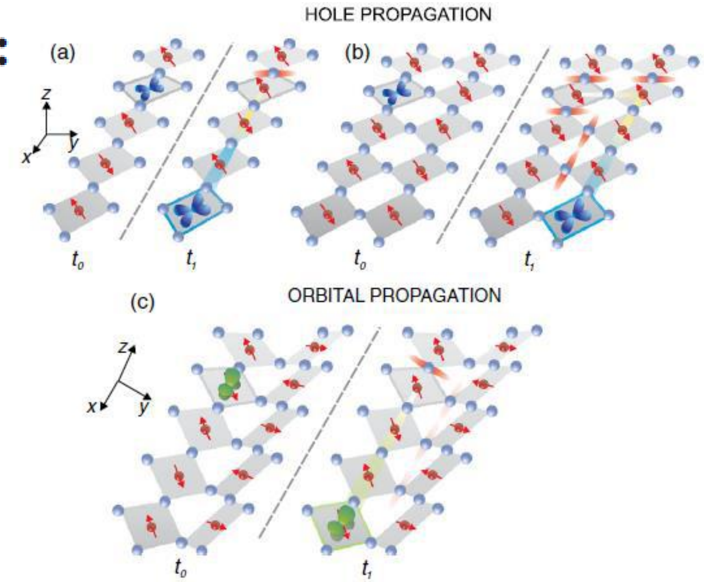

FIG. 1 (color online). Schematic view of the hole or orbiton propagation in an $S = 1/2$ environment. (a) A hole with $3d_{x^2-y^2}$ symmetry moves from its original position (second plaquette

$$\mathcal{H} = -J_{\mathrm{leg}}^{xz} \sum_{\langle \mathbf{i},\mathbf{j}\rangle \| x,\sigma} (o_{\mathbf{i}\sigma,xz}^{\dagger} o_{\mathbf{j}\sigma,xz} + \mathrm{H.c.}) + E_0^{xz} \sum_{\mathbf{i}} n_{\mathbf{i},xz}$$

$$+ J_{\mathrm{rung}} \sum_{\langle \mathbf{i},\mathbf{j}\rangle \| y} \mathbf{S_i} \cdot \mathbf{S_j} + J_{\mathrm{leg}} \sum_{\langle \mathbf{i},\mathbf{j}\rangle \| x} \mathbf{S_i} \cdot \mathbf{S_j}.$$

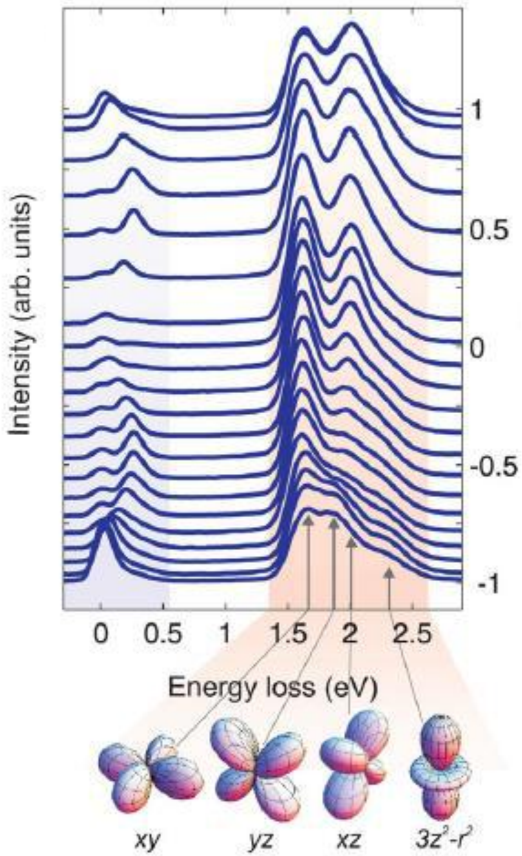

RIXS spectra of $CaCu_2O_3$

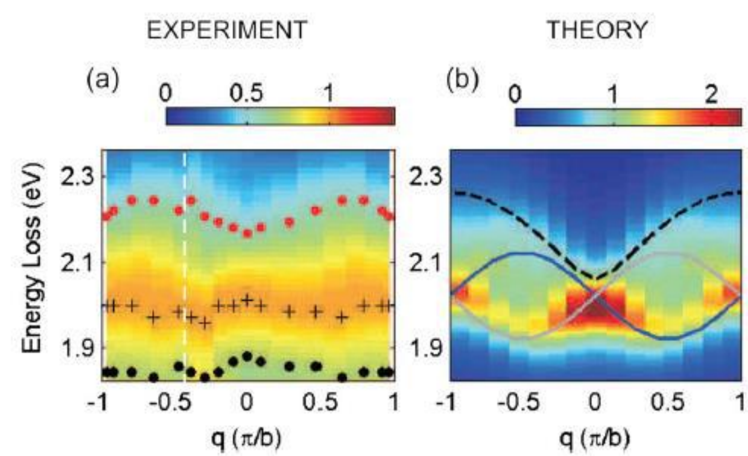

Jahn-Teller Effect in Systems with Strong On-Site Spin-Orbit Coupling

Conclusions.—We analyzed here the impact of a lattice-mediated Jahn-Teller effect in the presence of strong SOC, which quenches orbital degeneracy in the ground state.

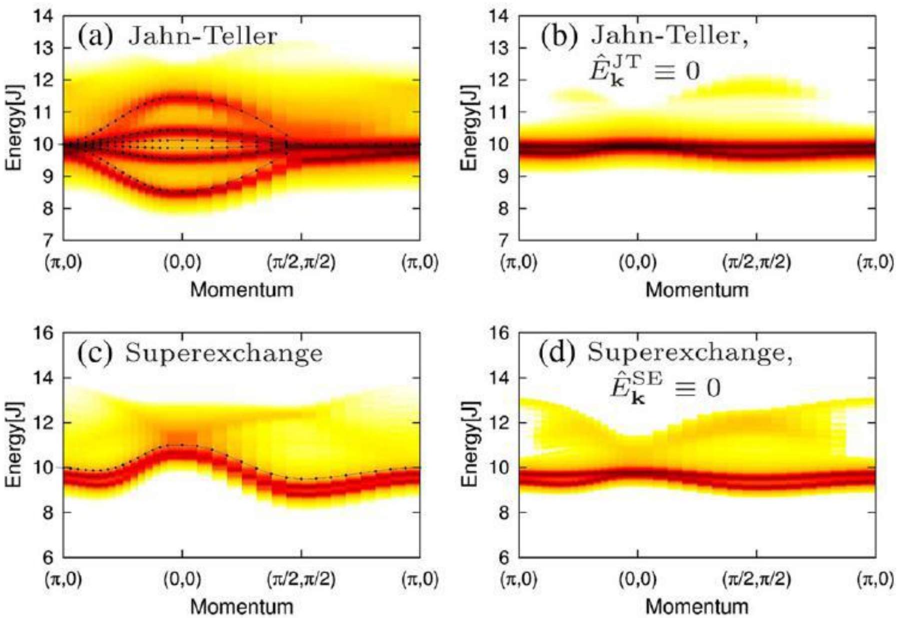

FIG. 3. Spin-orbit exciton spectra with propagation driven by either superexchange *or* Jahn-Teller interaction (calculated SCBA

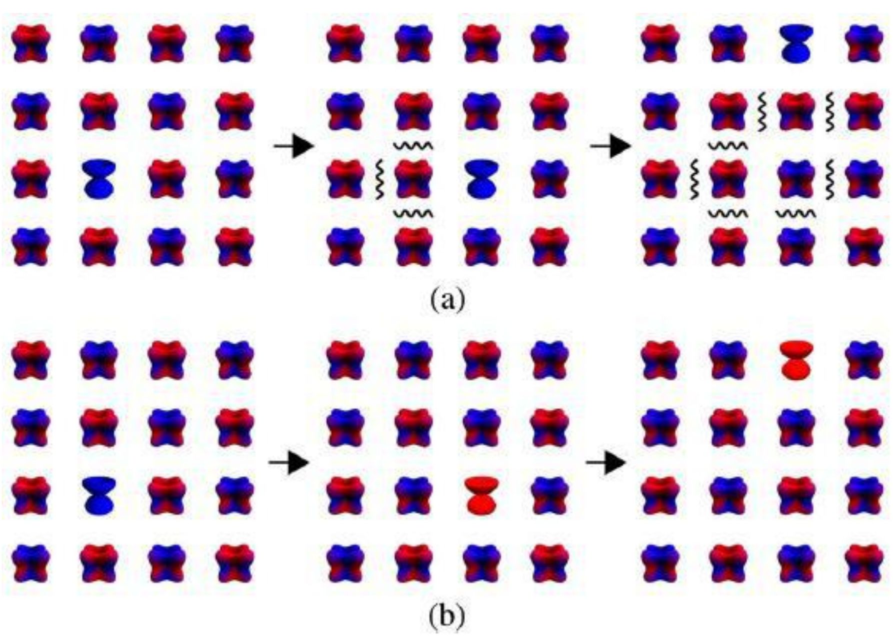

FIG. 4. Illustration showing the two types of nearest-neighbor hopping of a $j_{\rm eff} = 3/2$ exciton in the antiferromagnetically ordered background. (a) Polaronic hopping (due to Jahn-Teller effect *or* superexchange): a $j_{\rm eff} = 3/2$ exciton with the $j_z = -3/2$ quantum number (left-hand panel) does not change its j_z

SOE 18 Sep

[E.M. Plotnikova *et al*., PRL **116**, 165102 (16)]

Spin-orbital entanglement in Mott insulators

1. From Ising via e_g to 2D compass: increasing frustration
2. Kanamori parameters: Hubbard U and Hund's J
3. Goodenough-Kanamori rules: complementarity
4. Kugel-Khomskii e_g model in 3D and in 2D: QCP
5. Entanglement in spin excitations
6. Spin-orbital entanglement in t_{2g} models
7. Spin-orbital entanglement in Kitaev-Heisenberg model
8. Experimental consequences

e_g orbital order below $\boxed{T_c = 0.3566 \pm 0.0001}$

$$\boxed{T_c^{\text{Ising}} = \frac{1}{2\log(1+\sqrt{2})} \approx 0.567296.}$$

Thank you for your kind attention !

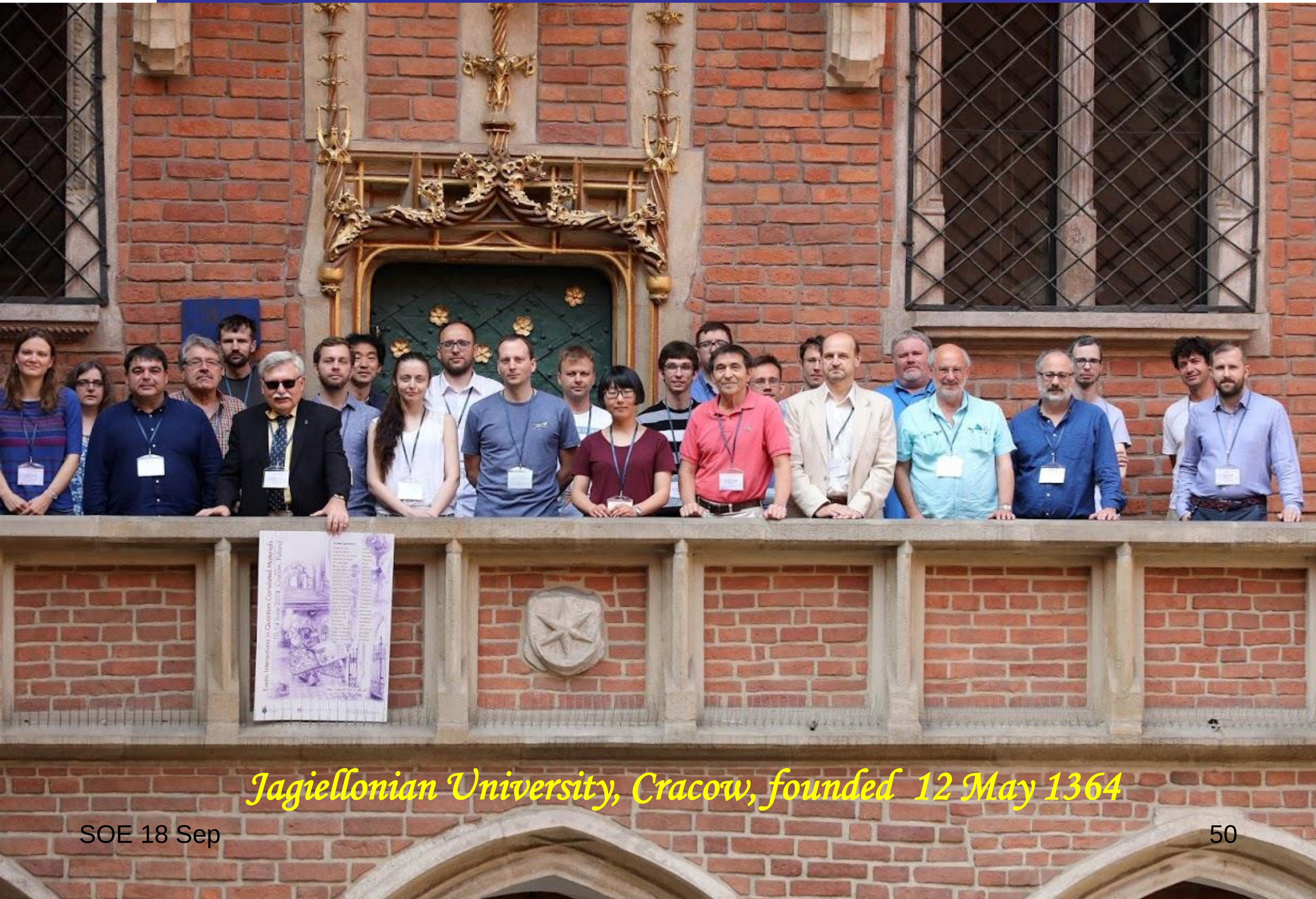

Jagiellonian University, Cracow, founded 12 May 1364